Gundi *et al. Helgol Mar Res* (2020) 74:8
https://doi.org/10.1186/s10152-020-00540-x

Helgoland Marine Research

ORIGINAL ARTICLE Open Access

Giant planktic larvae of anomalan crustaceans and their unusual compound eyes

Paula Gundi†, Chiara Cecchin†, Lara-Leonie Fetzer†, Carolin Haug, Roland R. Melzer and Joachim T. Haug*

Abstract

Crustacean larvae are usually recognised as small organisms, below one millimeter body size. However, in different crustacean groups such as Stomatopoda, Polychelida, or Achelata, also very large larvae occur with sizes of 20 mm and beyond. Also from few meiuran species ("short-tailed" crustaceans, including crabs, hermit crabs, or squat lobsters), rather large larvae are known, though still considerably smaller than 20 mm. We present here two specimens of anomalan meiuran larvae, each with a total length of 24 mm, which by far exceed the previously known/reported maximum sizes of meiuran larvae. Yet, both specimens exhibit characters that indicate their identity as zoea larvae (first larval phase with several stages), most likely shortly before the metamorphosis to the megalopa (second larval phase with one stage). Due to this early developmental state, it is difficult to provide a narrower systematic identification of the larvae. In addition to the description of the developmental status of all appendages, we also investigated the gizzard and especially the compound eyes. The latter possess a mixture of hexagonal, intermediate, and square-shaped facets in an unusual arrangement. We documented the exact arrangement of the facets in both specimens and discuss the possible re-structuring during metamorphosis. The arrangement of the different types of facets indicates that transformation to an adult eye structure takes place over several moults and that the facets are being rearranged in this process. The findings demonstrate that also meiuran larvae contribute to the fraction of the macro-plankton.

Keywords: Zoea, Anomala, Metamorphosis, Ommatidia, Plankton

Introduction

The larval forms of numerous crustaceans, especially those of Decapoda (prawns, shrimps, lobsters, crabs, and their relatives), represent an important part of the 'metazoan fraction' of the plankton. Size-wise many of these larvae are attributed to the micro-plankton (or meso-plankton, depending on the used scheme; e.g. [1–3]), yet there are also significantly larger forms that are part of the macro-plankton (or mega-plankton, also depending on the used scheme; e.g. [1–3]), hence larger than 20 mm in total body length.

Larvae reaching more than 20 mm of total body length occur in various crustacean groups (reviewed in [4]). Most prominent examples occur in three groups:

1. Achelata (slipper lobsters, spiny lobsters), with about 150 mm leg span, e.g. [5]);
2. Polychelida (deep-sea lobster-like crustacean) with overall lengths of about 100 mm (e.g. [6–8]);
3. Stomatopoda (mantis shrimp [9]) with larvae of about 50 mm in length (e.g. [10, 11]).

Furthermore, certain species of Meiura, the "short-tailed" crustaceans such as crabs, hermit crabs, and squat lobsters, have rather large larval forms (e.g. [12]), yet do not quite reach 20 mm in overall to be considered to represent macroplankton.

*Correspondence: jhaug@biologie.uni-muenchen.de
†Paula Gundi, Chiara Cecchin and Lara-Leonie Fetzer contributed equally
Ludwig-Maximilians-Universitat Munchen, Munich, Germany

Meiuran crustaceans possess a large variety of different larval forms with very different morphologies. Meiura includes the two sister groups Anomala and Brachyura (true crabs). Anomala includes very heterogeneous forms regarding their body shapes, lifestyles and habitats, including benthic deep-sea inhabitants, pelagic forms, and even terrestrial species [13]. Among others, Anomala includes hermit crabs, false crabs, and squat lobsters [12]. As a remark, different authors address the group 'Anomala' as 'Anomura', yet this term is more ambiguous as it has been used to refer to axiid and gebiid thalassinideans as well [14].

The majority of anomalan crustaceans, similar to most other forms of Decapoda, develop through a series of planktic larval stages, termed 'zoeas', followed by a morphologically and behaviourally transitional form, the megalopa stage (e.g. [15, 16]). This larva uses its pleopods (appendages of the posterior trunk) to swim and can already walk on its thoracopods, similar to juvenile and adult individuals. With these very different morphologies, each individual undergoes an extreme transformation from larva to adult. Such a process of transformation—often referred to as 'metamorphosis'—is a drastic change in the morphology of an organism during a short period of the post-embryonal development (see recent summary and variation of the application of the term in [17]).

One complex structure that has to change during metamorphosis is the compound eye. It develops from an apposition eye (specialised for well-lit surroundings) in the larva to a superposition eye (specialised for less well-lit surroundings) in the adult (e.g. [18]). Comparable transitions in holometabolous insects are mediated by a resting stage (pupa) allowing for drastic restructuring. Anomalan crustaceans lack such a pupa-like stage, their eyes have to retain overall functionality during the restructuring process.

The larval apposition eye represents a plesiomorphic morphology (for Euarthropoda in general) optimised for well-illuminated habitats with the typical hexagonal shape of the facets. Superposition eyes are specialised for dimmer habitats [19]. Within Anomala different types of superposition eyes are known: parabolic superposition, refracting superposition, and reflective or mirror superposition eyes [20]. The latter type is widespread throughout adults of Decapoda and is characterised by square-shaped facets.

In consequence, a compound eye covered with hexagonal facets needs to be transformed during ontogeny into one covered with square-shaped facets. It remains so far largely unclear how this process exactly takes place. In principle, there are two options:

1. Adult ommatidia are new structures and larval ommatidia become reduced; such a complete replacement seems present in certain insects [21, 22] or mantis shrimps [23].
2. Alternatively, ommatidia with hexagonal facets could be rearranged onto a square-type pattern; a comparable stage-specific transformation of individual ommatidia during ontogeny has been described for certain insects [24]. In the phantom midge, *Chaoborus crystallinus*, the larvae already possess true compound eyes, unlike most other larval holometabolous insects. The larval ommatidia are adapted to vision under water but are transformed during metamorphosis to ommatidia adapted to vision in air. This transformation involves cornea lenses and crystalline cones and provides the basic requirement for "neural pooling", a type of superposition that works very well under scotopic conditions (low light conditions; [25]).

Here we present two unusual larval specimens of anomalan crustaceans found in a museum collection. Both specimens are very large, more than 20 mm body length, with this representing the largest larval forms of meiuran crustaceans known so far. These giant larvae both show a mixture of square-shaped and hexagonal ommatidia in their compound eyes. This suggests that they are in a late stage of their larval development, shortly before the transition into the megalopa stage. Due to this early developmental state, it is difficult to provide a narrower systematic identification of the larvae. We provide a detailed description of the two anomalan specimens and discuss their developmental state. Despite the uncertainties about the systematic identities of the larvae, these larvae are so unique in their morphology that they provide new insights into two important aspects: (1) the metamorphosis of anomalan crustaceans, including the transformation of the eye from an apposition eye to a superposition eye, and (2) the evolution of giant larvae.

Materials and methods

Material

The two larval crustaceans used for this study came from the Musée National d´Histoire Naturelle in Paris. Specimen A was originally labeled as CARIDE II St. 113 (Pacific ocean, 0°00, 153°13°′W, 830 m depth, 19NOV1968). The official collection number of this specimen is now MNHN-IU-2014-5455. Specimen B was originally labeled as CARIDE V St.41 (Pacific ocean, navire océanographique "Coriolis", 10°0′S, 142°0′W, 575 m depth, 14SEP1969). The official collection number of this specimen is now MNHN-IU-2014-5466. Both seem to have been originally fixed in formaldehyde

(making molecular identification challenging to impossible), but have been transferred and are now stored in 70% ethanol.

Preparation

For documentation of the entire specimens, those were fixed with coverslips and metal nuts in 70% ethanol. After intensive documentation of the intact specimens, these were dissected using different preparation tools, such as needles and micro-scissors. The detached structures were documented separately and are now stored in individual Eppendorf-type cups with screw lids.

Documentation methods

The entire documentation process was performed with entire specimens or parts of them, which were emersed in their original storage liquid, 70% ethanol, to avoid drying out or damaging of the specimens to retain the possibility of further investigations. Different approaches were applied:

1. Entire specimens were documented with a Canon EOS Rebel T3i digital camera and Canon MP-E 65 mm lens. A Canon Macro Twin Lite MT-24EX flash was used for illumination. Specimens were fixed with a microscope coverslip on a black surface to avoid movement during the photographic process. To reduce the reflections caused by the flash, two polarizers were used in front of the two flashlights and one perpendicular polariser in front of the lens of the camera [26, 27]. Images were recorded from dorsal (Fig. 1a, b), ventral (Fig. 2a, b), and from the left lateral side (Fig. 3a, d).
2. Further documentation of entire specimens was performed on a Keyence BZ-9000 fluorescence microscope with 2×, 4× and 10× objectives (resulting in about 20×, 40× and 100× magnification). Autofluorescence imaging has certain advantages over transmitted white light microscopy ([6, 7, 28, 29]; Figs. 4a, b, 5a, b, 18a, b; excitation wavelengths: 470 nm/GFP, 358 nm/DAPI). Also, here specimens were fixed with coverslips and metal nuts.
3. Each image detail was documented with a stack, creating a series of images with consecutive focus.
4. Several image details had to be recorded due to the size of the two specimens to create one entire image of a specimen or structure.
5. After dissection, individual structures of the specimens were further documented on the same microscope with 2×, 4×, 10× and 20× objectives (resulting in about 20×, 40×, 100× and 200× magnification). Also, here auto-fluorescence capacities were exploited. Some structures were additionally documented under bright field or phase contrast settings.
6. For a higher resolution of small structures, like setae and setules, the specimen was documented on the same microscope with a 60× oil immersion objective. Also, here each image detail was documented with a stack of images with consecutive levels of focus. Image details with weak fluorescence were recorded a second time and sometimes also a third time with longer exposure times [30].

Data processing

1. Image stacks for each image detail were fused with CombineZM/ZP into consistently sharp images [27, 31].
2. Resulting sharp images were stitched to panorama images either with Adobe Photoshop CS3, 4 or 5, or Adobe Photoshop Elements 11.
3. For adding information from overexposed images, the image was placed in Adobe Photoshop as a separate layer above the image with shorter exposure time. The magic wand tool was used to mark overexposed areas; a feather with a high radius was applied to the edge, then these overexposed areas were cut out. The resulting image shows all parts well illuminated [30].
4. Finally, the images were edited in Adobe Photoshop CS 2 and CS 4, including optimization of the histogram and sharpness, manual removing of dirt particles and background, manual brightness, and contrast adjustments.
5. For highlighting certain structures on overview and detail images these were marked using a lasso tool and colourized with the colour balance tool on a separate layer, preserving the original shading.
6. To illustrate the opening angles of the ommatidia of the compound eyes, the projections of ommatidia rows and the pattern of the ommatidia arrangement, Adobe Illustrator CS2 and Adobe Photoshop CS2 were used for drawing schemes [32].

Results

The descriptive approach follows Haug [33]. Yet for convenience of the reader it is provided here as running text.

Description of specimen A

Habitus: Small euarthropodan larva with a strongly elongated and arched shield ("carapace") (Figs. 1a, 2a, 3a). Body differentiated into cephalothorax, pleon, and non-somitic telson and organised into 20 segments:

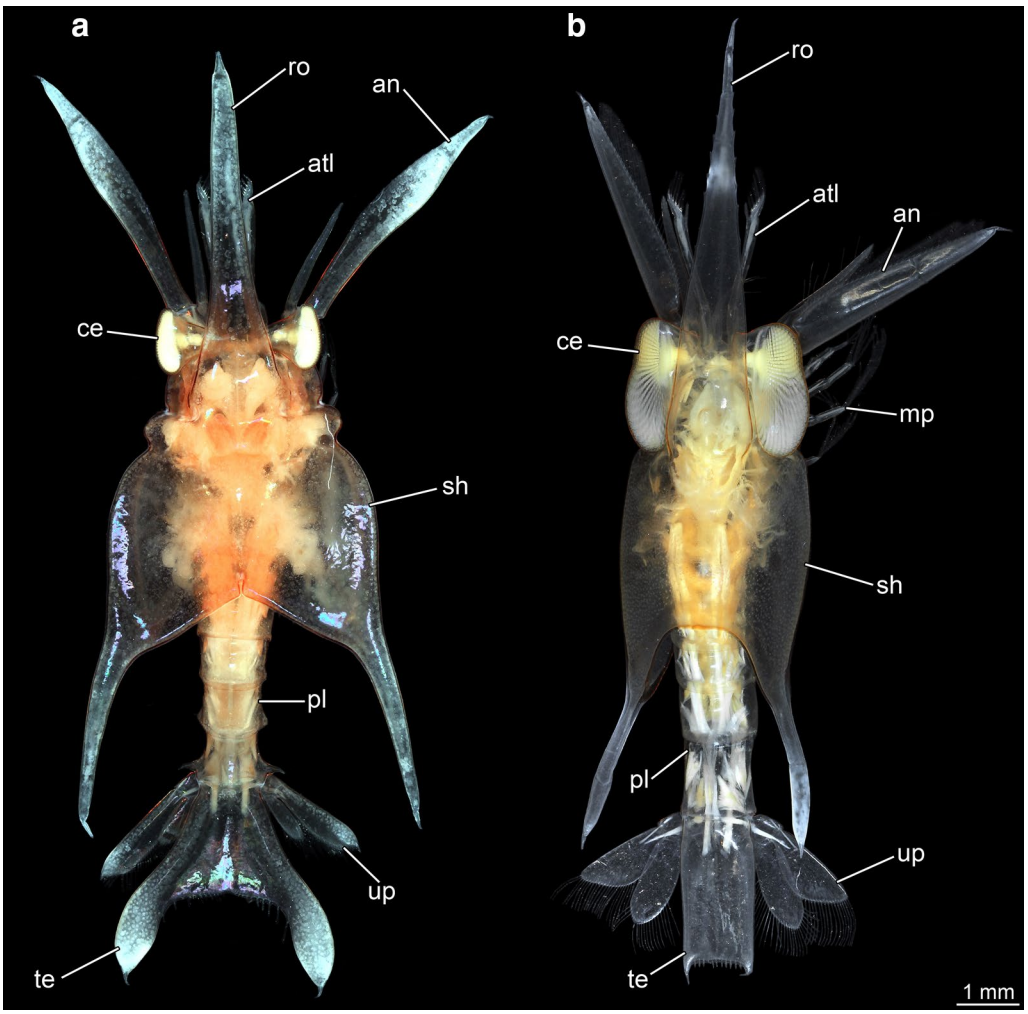

Fig. 1 Giant anomalan larvae, dorsal overviews, composite macrophotographic images (under cross-polarized light). **a** Overview of specimen A. **b** Overview of specimen B. *an* antenna, *atl* antennula, *ce* compound eye, *mp* maxilliped, *pl* pleon, *sh* shield, *te* telson, *up* uropods

ocular segment plus 19 appendage-bearing (post-ocular) segments. Ocular segment incorporated into the cephalothorax, the dorsal area contributes to the shield. Post-ocular segments 1 to 13 incorporated into the cephalothorax, their dorsal areas contribute to the shield.

Post-ocular segments 14 to 19 are all separate pleon segments, each dorsally forming a tergite.

Cephalothorax: Shield in dorsal view large and prominent and occupying 4/5 of the total length of the larva (observing overall length including all protruding structures) (Fig. 4b). Anterior rim of the shield drawn out into a very prominent rostrum. Rostrum elongated triangular-shaped, occupying less than ½ of the total length of the larva; longer than wide, about 4×, with no spines present. With two distinct structures: a trapezoidal field with 4 pores positioned after about 1/6 of the rostrum length (Fig. 5b, e) and muscle attachment depressions as 2 distinct lines in v-shape.

Main part of shield more or less trapezoidal in dorsal view, longer than wide, about 1.4×, with a flat v-shaped notch at the posterior rim. A cleft in the middle of the posterior rim continues into a keel almost reaching the muscle attachment structures. Postero-lateral edges drawn out into 2 long spines; longer than wide, about 4×, and longer than the main part of the shield, about 1.3×.

Surface of the shield with 3 distinct pairs of ridges extending from anterior to posterior: a lateral ridge, a latero-ventral ridge, and a ventral ridge. Lateral ridge outlines the lateral margins of the shield, extending from the base of rostrum, posteriorly emanating into the postero-lateral spines and forming a short wing-like structure. Latero-ventral ridge extends from a protrusion positioned laterally, posteriorly to the base of the

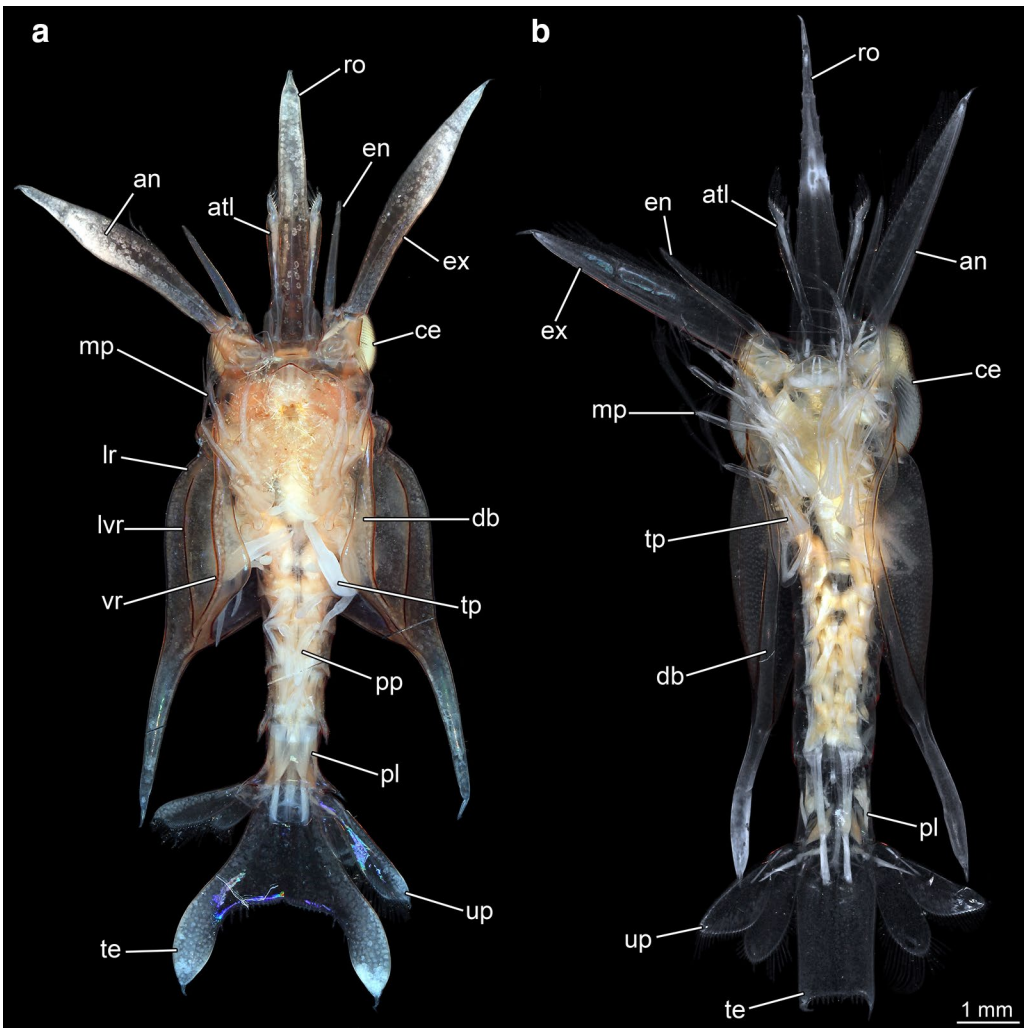

Fig. 2 Giant anomalan larvae, ventral overviews, composite macrophotographic images (under cross-polarized light). **a** Overview of specimen A. **b** Overview of specimen B. *an* antenna, *atl* antennula, *ce* compound eye, *db* doublure, *en* endopod, *ex* exopod, *lr* lateral ridge, *lvr* latero-ventral ridge, *mp* maxillipeds, *pl* pleon, *pp* pleopods, *ro* rostrum, *te* telson, *tp* thoracopods, *up* uropods, *vr* ventral ridge

postero-lateral spines. Ventral ridge extends from the region ventral to the protrusion laterally, posteriorly to the base of the postero-lateral spines; marking the effective ventral outline of the shield; extending into well-developed doublure. Ventral edge with small teeth.

Dorsal surface of shield with a circular field positioned in the middle of the posterior part of the shield; consisting of 6 pores; 2 pores situated posterior of the circular field (Fig. 5b, f).

Overall surface of shield with small (possibly sensorial) setae dorsally and ventrally; dorsally more numerous than ventrally.

Pleon (Figs. 4a, b, 5a, b) Tergite of post-ocular segment 14 (pleomere 1) roughly rectangular in dorsal view, anterior rim convex. With one spine on each lateral side (possible precursor structures of the tergopleura); postero-lateral edges of tergite continuous to the ventral sclerotisation (sternite).

Tergite of post-ocular segment 15 (pleomere 2) rectangular in dorsal view; more than twice as wide as long; about 2/3 of the length of preceding segment and slightly narrower. With one spine on each lateral side (possible precursor structures of the tergopleura). Postero-lateral edges of tergite continuous with the ventral sclerotisation (sternite).

Tergite of post-ocular segment 16 (pleomere 3) rectangular in dorsal view; wider than long, about 2×; slightly longer and slightly narrower than preceding segment. With one spine on each lateral side (possible precursor structures of the tergopleura). Postero-lateral edges

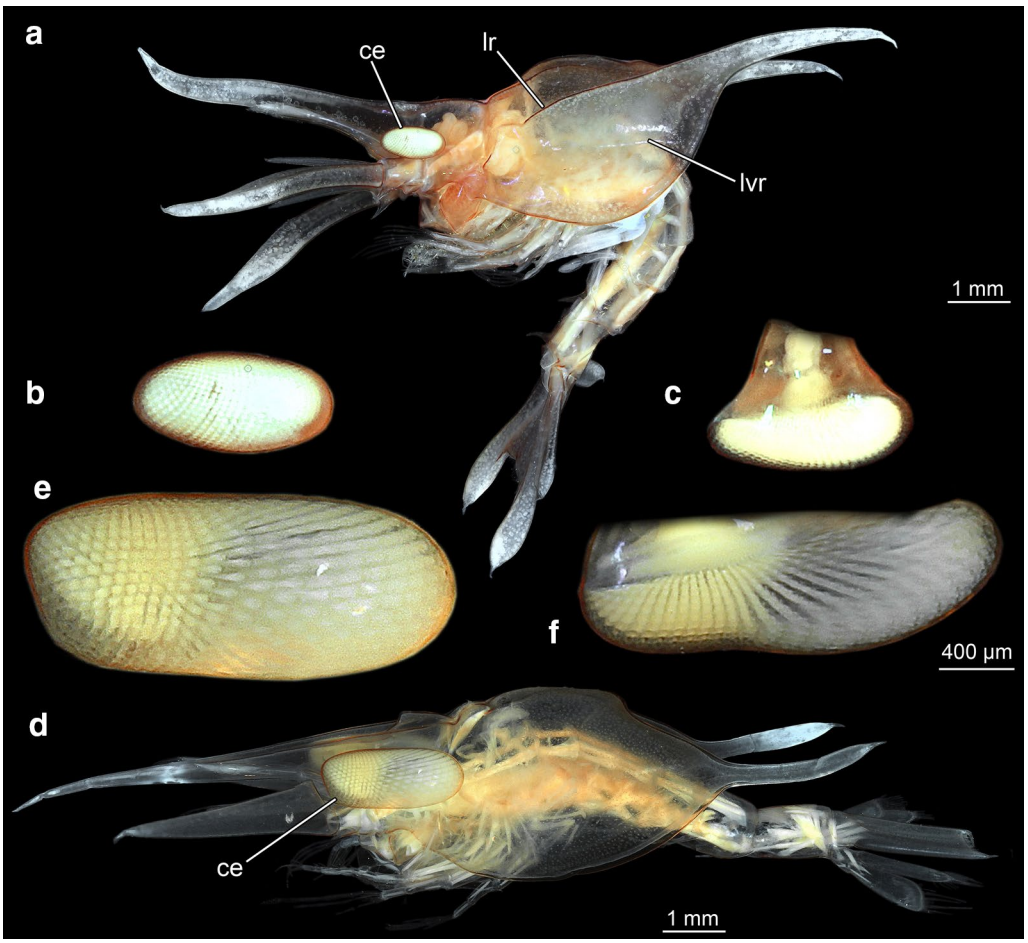

Fig. 3 Lateral overviews of entire specimens and details of compound eyes, composite macrophotographic images (under cross-polarized light). **a**–**c** Specimen A. **a** Overview in lateral view. **b** Compound eye in dorsal view. **c** Compound eye in lateral view. **d**–**f** Specimen B. **d** Overview in lateral view. **e** Compound eye in lateral view. **f** Compound eye in dorsal view. *ce* compound eye, *lr* lateral ridge, *lvr* latero-ventral ridge

of tergite continuous with the ventral sclerotisation (sternite).

Tergite of post-ocular segment 17 (pleomere 4) rectangular in dorsal view; wider than long, about 1.5×; longer than preceding segment, about 1.3×, slightly narrower. With one spine on each lateral side (possible precursor structures of the tergopleura). Postero-lateral edges of tergite continuous with the ventral sclerotisation (sternite).

Tergite of post-ocular segment 18 (pleomere 5, Fig) square-shaped in dorsal view; longer than preceding segment, about 1.3×, also narrower. With one elongated prominent spine on each lateral side (possible precursor structures of the tergopleura). Postero-lateral edges with tergite continuous with the ventral sclerotisation (sternite).

Tergite of post-ocular segment 19 (pleomere 6) square-shaped in dorsal view; slightly longer and less wide than preceding segment. With one elongated prominent spine on each lateral side (possible precursor structures of the tergopleura). Postero-lateral edges with tergite continuous to the ventral sclerotisation (sternite). Surface of all segments with (sensorial?) setae in dorsal and ventral view; dorsally more than ventrally.

Telson: Trapezoidal in dorsal view and drawn out into a paddle-shaped extension of the lateral rim on each side, each with a spine distally (Figs. 1a, 2a, 4a, b, 5a, b). About as long as wide; with distinct median indentation.

Posterior rim bearing 10–11 spine-like setae on each side of the indent differing in length and width. Surface covered with (sensorial?) setae in dorsal and ventral view; dorsally more numerous than ventrally. The anal opening not visible.

Ocular segment: Bearing a pair of compound eyes, each one inserting laterally (Fig. 5a–d). Each compound eye differentiated into proximal stalk and distal cornea. Corneal region with distinct facets, indicating ommatidia. Length of compound eye about 1/15 of the total length

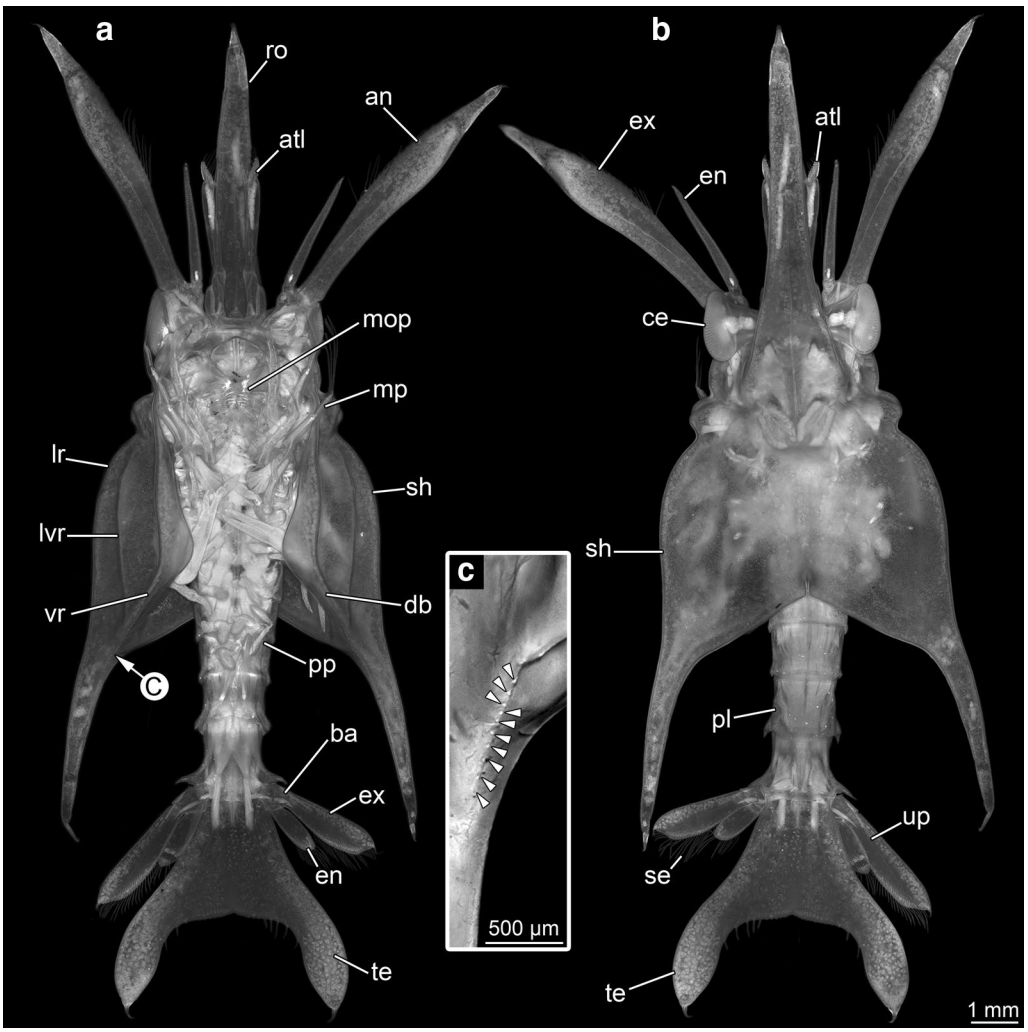

Fig. 4 Overview images of specimen A, autofluorescence images (**a**, **b** 470 nm, **c** 358 nm). **a** In ventral view. **b** In dorsal view. **c** Close-up on ventral teeth (arrowheads). *an* antenna, *atl* antennula, *ba* basipod, *ce* compound eye, *db* doublure, *en* endopod, *ex* exopod, *lr* lateral ridge, *lvr* lateroventral ridge, *mop* mouth parts, *mp* maxillipeds, *pl* pleon, *ro* rostrum, *se* setae, *sh* shield, *te* telson, *up* uropods, *vr* ventral ridge

of the larva. Compound eye in dorsal view more or less bean-shaped with straight lateral side, longer than wide, about 3×, only considering ommatidia region. With triangular pore field dorsally at the stalk (Fig. 6a, d). Compound eye in lateral view oval-shaped, longer than wide, about 2×. Ommatidia arranged in 36 ommatidia rows from anterior to posterior (rows strongly curving anteriorly and posteriorly). There are about 20 ommatidia in each row in the middle; anterior and posterior with fewer ommatidia per row. Facets are shaped hexagonal, square-shaped, or intermediate; an area with square-shaped ommatidia mostly anterior-ventrally positioned in row 9 to 22; around this area facets of intermediate shape (Fig. 7a).

Hypostome-labrum complex with a triangular labrum (ventral view) with the tip pointing towards the anterior part (wider than long, about 2×).

Appendage of post-ocular segment 1 (antennula): Generally differentiated into peduncle and 2 flagella (Figs. 8a–f, 9a–d, i); about half the size of the rostrum. Peduncle tube-shaped and subdivided into two discrete elements. Element 1 tube-shaped and occupies 1/4 of the total length; longer than wide, about 2×. Element 2 tube-shaped, longer than wide, about 5×; with 2 setulose setae medio-distally. Future subdivision of element 2 into two elements indicated by fold. Flagellum 1 (median) spine-like and not (yet) subdivided into ringlets. Flagellum 2 (lateral) more or less triangular in anterior–posterior

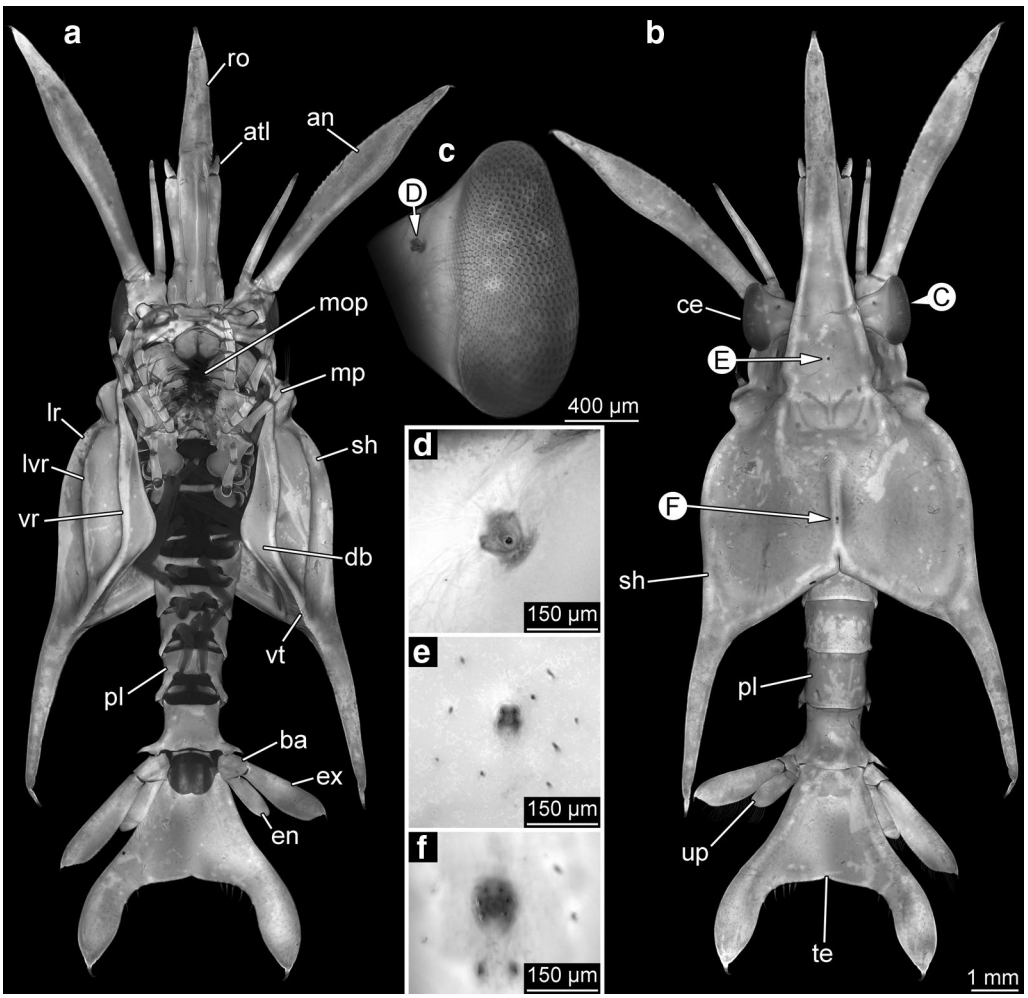

Fig. 5 Overview images and details of eyes and shield of specimen A, autofluorescence images (358 nm). **a** Overview in ventral view. **b** Overview in dorsal view. **c** Isolated eye in dorsal view. **d** Close-up on possible chemoreceptor of eye. **e** Close-up on possible sensory dorsal organ of rostrum. **f** Close-up on possible sensory organ of shield. *an* antenna, *atl* antennula, *ba* basipod, *ce* compound eye, *db* doublure, *en* endopod, *ex* exopod, *lr* lateral ridge, *lvr* latero-ventral ridge, *mop* mouth parts, *mp* maxillipeds, *pl* pleon, *ro* rostrum, *sh* shield, *te* telson, *up* uropods, *vr* ventral ridge, *vt* ventral teeth

view; larger than flagellum 1, about 2× and not (yet) subdivided into ringlets; with 9 setae medially.

Appendage of post-ocular segment 2 (antenna): Generally differentiated into coxa, basipod, endopod, and exopod (Figs. 8a, b, g–j, 9a, b, e–l). Antenna longer than preceding appendage, about 1.6×. Coxa trapezoidal in anterior–posterior view, wider than long, about 1.5×. No setae present.

Basipod more or less rectangular in anterior–posterior view; slightly longer than wide. Medio-lateral edge drawn out into a small spine. Postero-distal edge drawn out into a prominent spine. Proximo-lateral edge bearing one tube-shaped apophysis. Endopod arising medio-distally from the basipod; tube-shaped, tapering distally; slightly smaller than entire antennula. No setae present. Exopod arising latero-distally from the basipod; more or less tube-shaped, consisting of 1 element and a spine distally; multiple setae medially; longer than endopod, about 2× also wider about 3×. Surface with numerous (sensorial?) setae.

Appendage of post-ocular segment 3 (mandible): Not differentiated into substructures, represented only by coxa. Coxa medially forming gnathal edge, differentiated into pars molaris with 1 tooth and pars incisivus with 10 teeth (Figs. 10a, c, d, 11a, c, d). No clear distinction between pars molaris and pars incisivus of the left mandible (Fig. 12). Mandibular palp not visible. Sternal protrusion of mandibular segment (paragnaths)

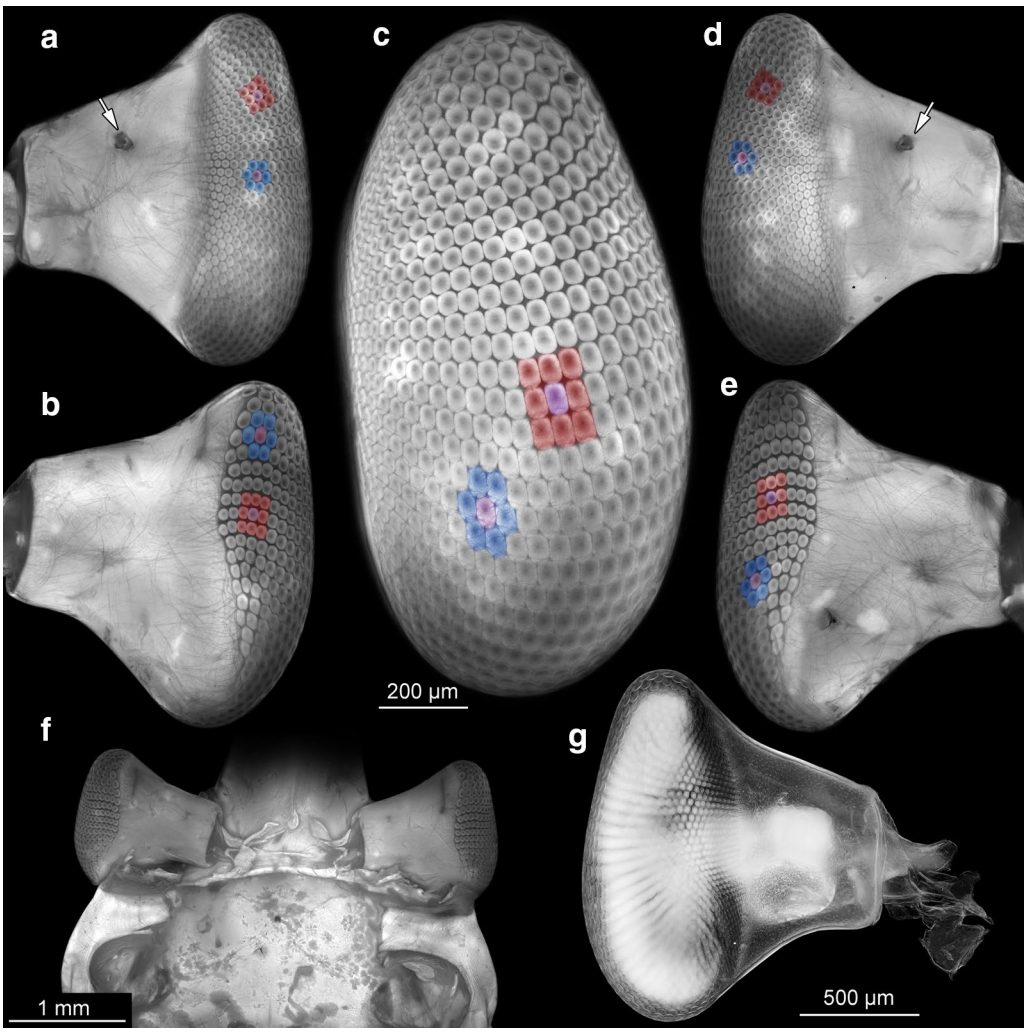

Fig. 6 Overview of eyes of specimen A. **a**–**f** Autofluorescence images (358 nm); note different shapes of facets: ommatidium (purple) surrounded by eight ommatidia (red) = squared arrangement; ommatidium (purple) surrounded by six ommatidia (blue) = hexagonal arrangement; arrows pointing to a possible chemoreceptor. **a**, **b** Colour-marked right eye. **a** Dorsal view. **b** Ventral view. **c**–**e**, **g** Colour-marked left eye. **c** Lateral view. **d** Dorsal view. **e** Ventral view. **f** Overview of eyes still in situ; ventral view. **g** Inverted white light image; dorsal view

more or less rounded triangular in anterior–posterior view, lobe-like with massive base; longer than wide, about 2×. Entire surface covered with small short setae.

Appendage of post-ocular segment 4 (maxillula): Generally differentiated into coxa, basipod, and endopod; slightly smaller than preceding appendage (Figs. 10a, e, f, 11a, e, f). Coxa medially drawn out into coxal endite; laterally forming distinct sclerite. Coxal endite paddle-shaped, curved, with about 9 setae distally; longer than wide, about 2×. Basipod trapezoidal in anterior–posterior view, medially drawn out into distinct endite; longer than wide, about 2.4×. Basipodal endite blade-like; wider than coxal endite, about 1.3×; with about 10 setae distally. Endopod arising medio-distally from the basipod; tube-shaped; about half as long as the coxal endite; with 4 setae distally.

Appendage of post-ocular segment 5 (maxilla):: Generally differentiated into coxa, basipod, endopod and exopod; slightly larger than preceding appendage (Fig. 10a, g, h, 11a, g-j). Coxa medially with 2 endites: Proximal coxal endite blade-shaped; with about 13 setulose setae; 11 setae evenly distributed along the median edge; 2 setae arising from the anterior surface of the endite; all pointing medially. Distal coxal endite tube-like, smaller than proximal coxal endite; with 4 setae; 1 seta on the median edge; 3 setae arising from the anterior surface of the endite; all pointing medially.

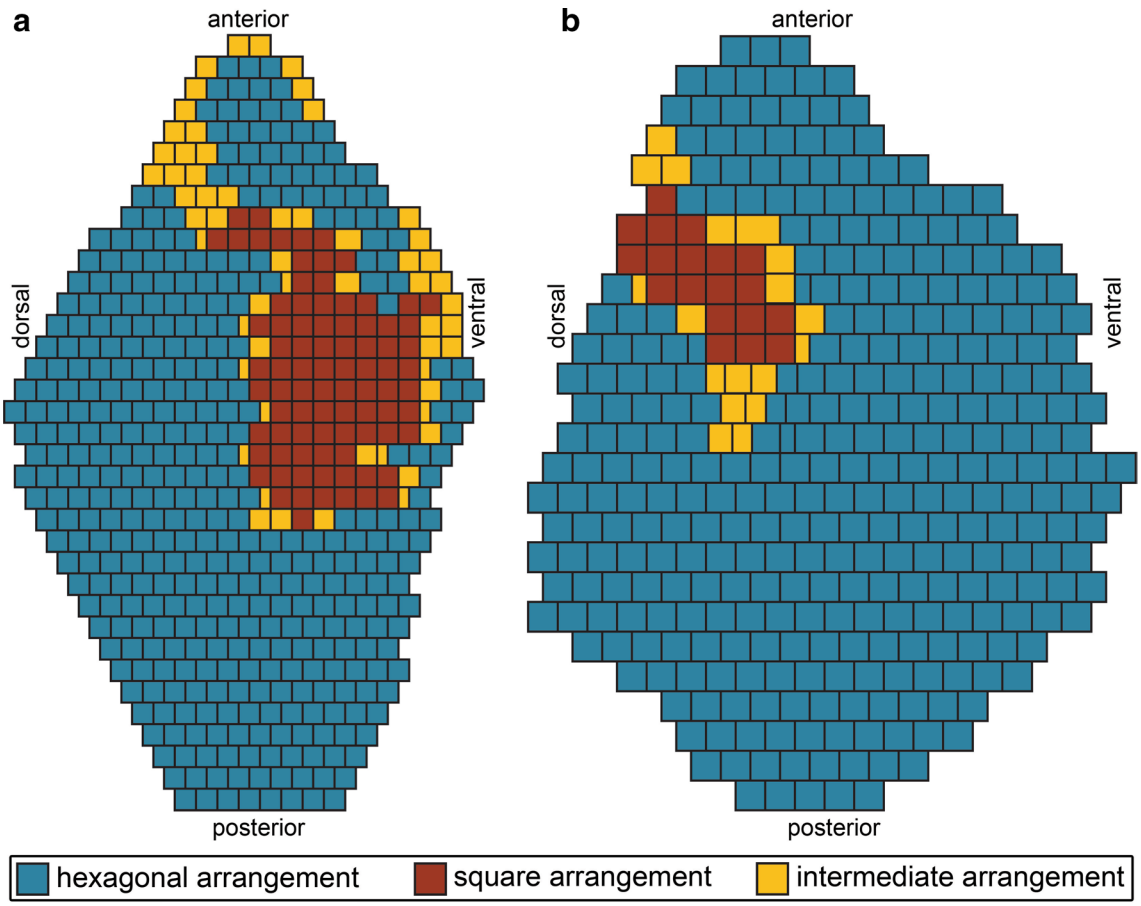

Fig. 7 Simplified mapping of facets on eye surface of specimen A (**a**) and specimen B (**b**). Rows of facets are depicted as straight, although anterior and posterior rows are strongly curved. Also shape is not directly represented (all facets are depicted as rectangles, independent of shape), but indirectly: hexagonal facets are surrounded by six other facets, intermediate facets by seven, and square-shaped ones by eight other facets. Also the original size differentiation of the facets is not represented

Basipod medially with 2 endites: Proximal basipodal endite with about 7 setae evenly distributed along the median edge; 1 seta arising from the anterior surface of the endite; all pointing medially.

Distal basipodal endite blade-like; slightly larger than proximal basipodal endite; about the same size as proximal coxal endite; with about 13 setae; 12 setae evenly distributed along the median edge; 1 setae arising from the anterior surface of the endite; all pointing medially.

Endopod arising medio-distally from the basipod; tube-shaped; longer than wide, about 4×; with about 8 setae; 3 setae evenly distributed along the median edge; 2 setae further proximal; 3 setae on the side towards the distal basipodal endite; all pointing medially. Exopod arising latero-distally from the basipod; prominent, lobe-like; 2 distinct regions are distinguishable: proximal region paddle-like; proximo-lateral edge of paddle extending into second fin-shaped region oriented towards the main body; with setulose setae around the entire rim.

Appendage of post-ocular segment 6 (maxilliped 1): Generally differentiated into coxa, basipod, endopod, and exopod Fig. 13a–c, 14a–d). Coxa differentiated into median and lateral sclerite. Further details not accessible; medially with 2 setae. Basipod rectangular in anterior–posterior view; longer than wide, about 2×; medially with 8 setae arranged in 4 groups, 1 group far proximally, 3 groups further distally.

Endopod arising medio-distally from the basipod; consists of 5 tube-shaped elements. Endopod element 1 (ischium) longer than wide, about 1.5×; with 1 seta medio-distally. Endopod element 2 (merus) longer than wide, about 1.5×; about the same size as element 1; with 2 setae medio-distally and 1 seta latero-distally. Endopod element 3 (carpus) slightly longer than wide; about the same size as element 2; with 1 seta medio-distally and 1 seta latero-distally. Endopod element 4 (propodus) about as long as wide; slightly smaller than element 3; no setae present. Endopod element 5 (dactylus) about as long as

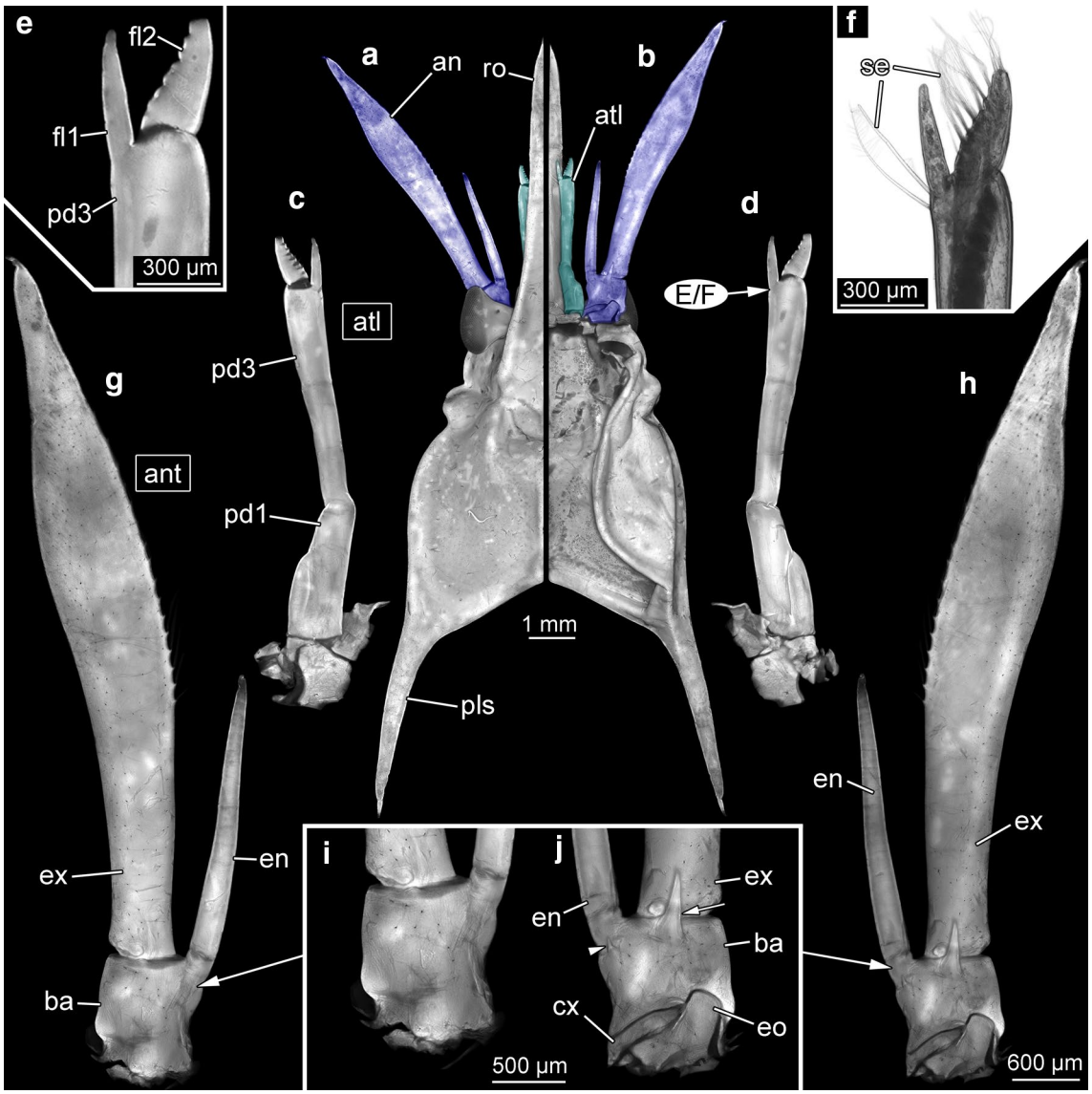

Fig. 8 Shield and anterior appendages of specimen A. Composite autofluorescence images (358 nm), besides F, which was recorded under transmitted white light conditions. Combined dorsal (**a**) and ventral (**b**) view of anterior cephalothorax; colour-marked antennula (cyan) and antenna (blue). **c**, **g**, **i** Anterior view. **d**–**f**, **h**, **j** Posterior view. **c**, **d** Isolated left antennula. **e**, **f** Close-up on flagella of left antennula. **g**, **h** Isolated left antenna. **i**, **j** Close-up on coxa and basipod of left antenna; note large spine (arrow) and small spine (arrowhead). *an* antenna, *atl* antennula, *ba* basipod, *cx* coxa, *en* endopod, *eo* excretory opening, *ex* exopod, *fl1, 2* flagellum 1, 2, *pd 1–3* peduncle 1–3, *pls* postero-lateral spine, *ro* rostrum, *se* setae

wide; slightly smaller than element 4; no setae present. Exopod arising latero-distally from the basipod; tube-shaped; with 2 prominent elements proximally and a distal region subdivided into 3 ringlets; longer than wide, about 4×; slightly shorter than endopod; with about 5 setae distally arising from the 3 ringlets.

Appendage of post-ocular segment 7 (maxilliped 2): Generally differentiated into coxa, basipod, endopod and exopod; slightly smaller than preceding appendage (Fig. 13a, d, e, 14a, d, e). Coxa differentiated into median and lateral sclerite. Further details not accessible. Basipod rectangular in anterior–posterior view; slightly smaller than the basipod of preceding appendage; slightly longer than wide; medially with 3 setae arranged in 2 groups.

Endopod arising medio-distally from the basipod; consists of 5 tube-shaped elements. Longer than preceding appendage, about 1.5×. Endopod element 1 (ischium) slightly longer than wide; medio-distally with 2 setae

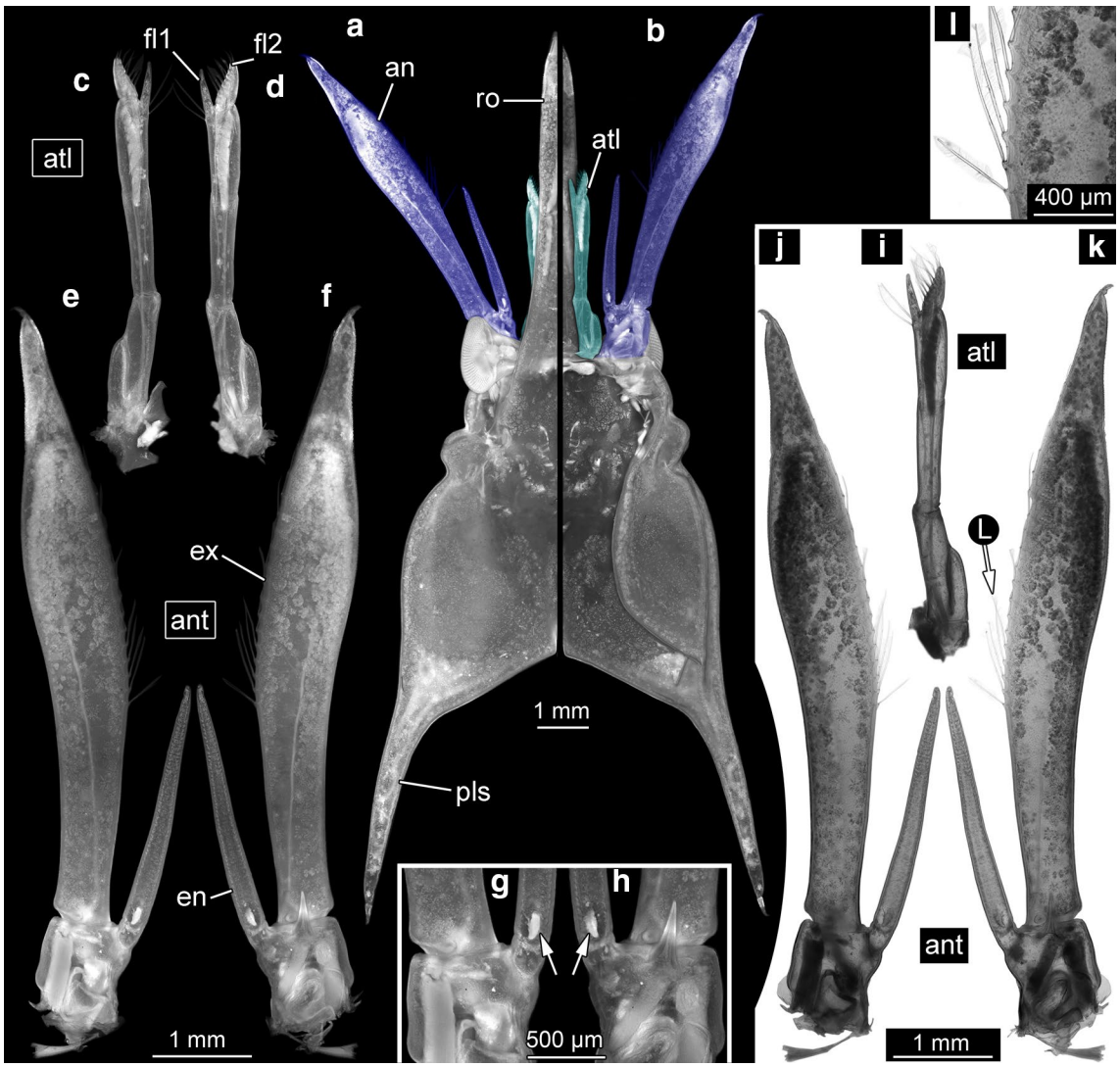

Fig. 9 Shield and anterior appendages of specimen A. **a**–**h** Composite autofluorescence images (470 nm). **i**–**l** Transmitted white light images. Combined dorsal (**a**) and ventral (**b**) view of anterior cephalothorax; colour-marked antennula (cyan) and antenna (blue). **c**, **e**, **g**, **j** Anterior view. **d**, **f**, **h**, **i**, **k**, **l** Posterior view. **c**, **d**, **i** Isolated left antennula. **e**, **f**, **j**, **k** Isolated left antenna. **g**, **h** Close-up on coxa and basipod of left antenna, arrow pointing to a possible statocyst. **l** Close-up of setae of left antenna. *an* antenna, *atl* antennula, *en* endopod, *ex* exopod, *fl1*, *2* flagellum 1, 2, *pls* postero-lateral spine, *ro* rostrum

arranged in 2 groups. Endopod element 2 (merus) longer than wide, about 1.5×; slightly longer than element 1; medio-distally with 2 setae arranged in 2 groups and 1 seta latero-distally. Endopod element 3 (carpus) continuous with element 4; about as long as wide; about half the length of element 2. with 1 seta medio-distally and 1 seta latero-distally. Endopod element 4 (propodus) about as long as wide; about the same size as preceding element; with 2 setae medio-distally. Endopod element 5 (dactylus) longer than wide, about 2×; not as wide as element 4; with about 3 setae distally and 1 seta medially.

Exopod arising latero-distally from the basipod; tube-shaped; longer than wide, about 5×; with 2 prominent elements proximally and a distal region subdivided into 3 ringlets; longer than endopod, about 1.5×; slightly longer than exopod of appendage 6, with about 4 setae distally arising from the 3 ringlets.

Appendage of post-ocular segment 8 (maxilliped 3): Generally differentiated into coxa, basipod, endopod and exopod; about 2/3 of the length and width of preceding appendage (Fig. 13a, f, g, 14a, f, g). Coxa differentiated into median and lateral sclerite. Further details not

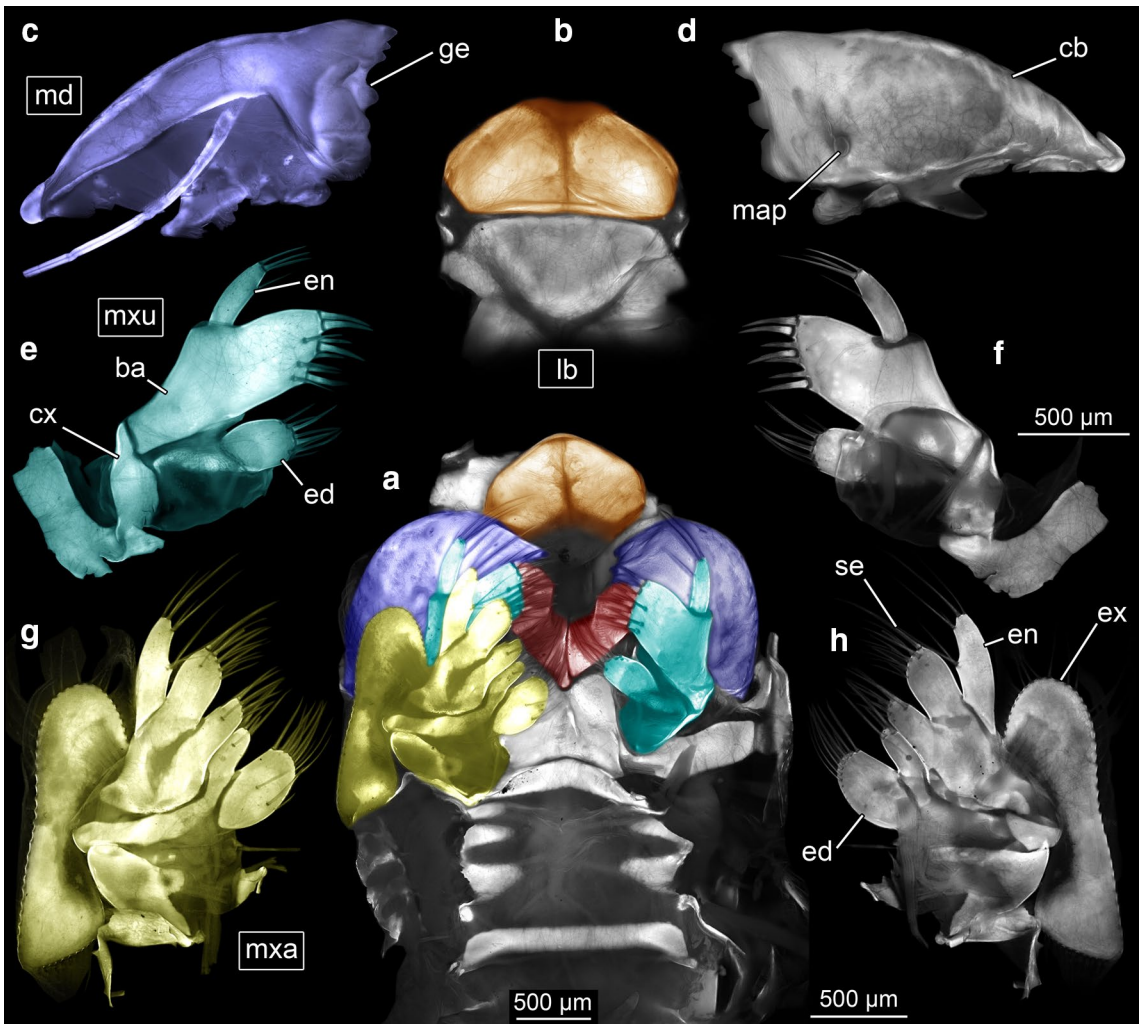

Fig. 10 Mouthparts of specimen A. Autofluorescence images (358 nm). **a** Colour-marked overview of mouthparts in situ in ventral view: labrum (orange), mandibles (violet), paragnaths (red), maxillulae (cyan), and maxillae (yellow). **b**–**h** Isolated mouthparts. **b**, **d**, **e**, **g** Posterior view (all right side except for mandible). **c**, **f**, **h** Anterior view (all right side except for mandible). **b** Labrum. **c**, **d** Mandible. **e**, **f** Maxillula. **g**, **h** Maxilla. *ba* basipod, *cb* coxal body, *cx* coxa, *ed* endite, *en* endopod, *ex* exopod, *ge* gnathal edge, *map* mandibular palp, *md* mandible, *mxa* maxilla, *mxu* maxillula, *se* setae

accessible. Basipod more or less triangular; longer than wide, about 1.5×.

Endopod arising medio-distally from the basipod; tube-shaped; distal part sclerotized, proximal part unsclerotized, soft; longer than wide, about 5×; future subdivision indicated. Exopod arising latero-distally from the basipod; tube-shaped; about 2/3 of the length of exopod of appendage 7; with 2 prominent elements proximally and a distal region subdivided into 3 ringlets; longer than wide, about 5×; about the same size of endopod; with about 4 setae distally arising from the 3 ringlets.

Appendage of post-ocular segment 9 (thoracopod 4): Weakly differentiated into 5 elements; 4 distal elements can be identified as ischium + merus, carpus, fixed finger (propodus) and moveable finger (dactylus); exact identity of 2 proximal elements unclear (Fig. 15a–e). Fingers about 1/3 of the size of thoracopod 4. Next layer of cuticle not visible. Appendage tube-shaped; fluorescence capacities different from maxillipeds (weaker). No setae present. Basipod not clearly distinguishable.

Endopod arising medio-distally from the basipod; tube-shaped; consists of 4 elements. Endopod element 1 (ischium) slightly curved; slightly wider than long. Endopod element 2 (merus) curved; longer than wide, about 3×; longer than preceding element, about 6×. Endopod element 3 (carpus) longer than wide, about 2×; about half the length of preceding element. Endopod element 4

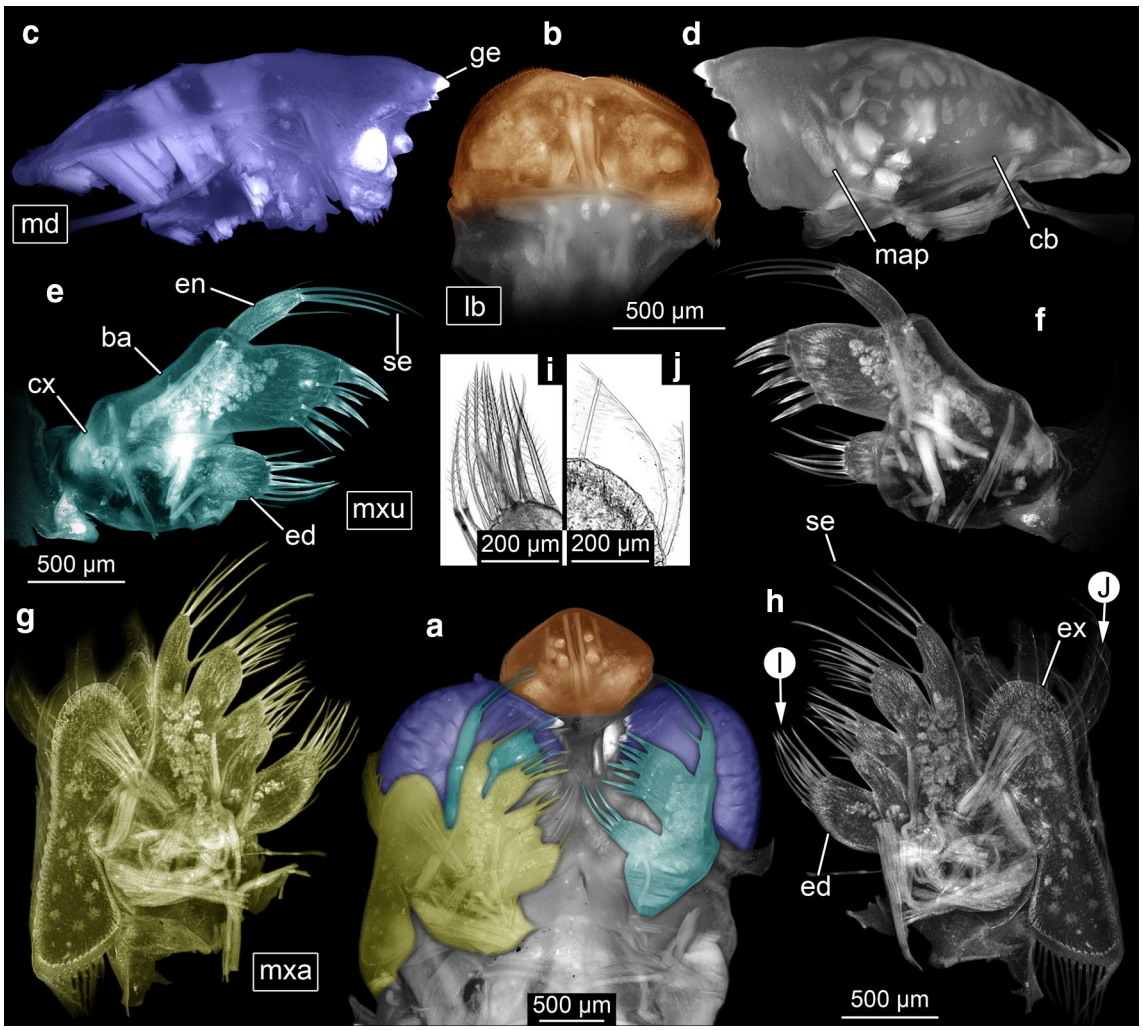

Fig. 11 Mouthparts of specimen A. Autofluorescence images (470 nm) besides I and J which were recorded under transmitted white light conditions. **a** Colour-marked overview of mouthparts in situ in ventral view: labrum (orange), mandibles (violet), maxillulae (cyan), and maxillae (yellow). **b**–**h** Isolated mouthparts. **b**, **d**, **e**, **g** Posterior view (all right side except for mandible). **c**, **f**, **h** Anterior view (all right side except for mandible). **b** Labrum. **c**, **d** Mandible. **e**, **f** Maxillula. **g**, **h** Maxilla. **i** Close-up of setae on maxillary endite. **j** Close-up of setae on maxillary exopod. *ba* basipod, *cb* coxal body, *cx* coxa, *ed* endite, *en* endopod, *ex* exopod, *ge* gnathal edge, *map* mandibular palp, *md* mandible, *mxa* maxilla, *mxu* maxillula, *se* setae

(propodus) distally drawn out into spine-like fixed finger. Fixed finger longer than wide, about 6×. The entire propodus longer than wide, about 5×; longer than preceding element, more than 3×. Endopod element 5 (moveable finger/dactylus) spine-like; longer than wide, about 6×; about the same size as fixed finger.

Appendage of post-ocular segment 10 (thoracopod 5): Weakly differentiated into 5 elements; 4 distal elements can be identified as ischium + merus, carpus, fixed finger (propodus) and moveable finger (dactylus); exact identity of 2 proximal elements unclear (Fig. 15a, b, f, g). Slightly shorter and half of the width of preceding appendage. Next layer of cuticle not visible. Appendage tube-shaped. Insertion area of the appendage located further dorsally than preceding appendage. Fluorescence capacities different from maxillipeds (weaker). No setae present.

Endopod arising medio-distally from the basipod; tube-shaped; consists of 4 elements. Endopod element 1 not (yet) differentiated into ischium and merus; longer than wide, about 3×. Endopod element 2 (carpus) slightly longer than wide; about 1/3 of the length of preceding element. Endopod element 3 (propodus) curved; longer than wide, about 3×; about twice of the length of preceding element. Endopod element 4 (dactylus) spine-like; longer than wide, more than 4×; longer than preceding element, about 2×.

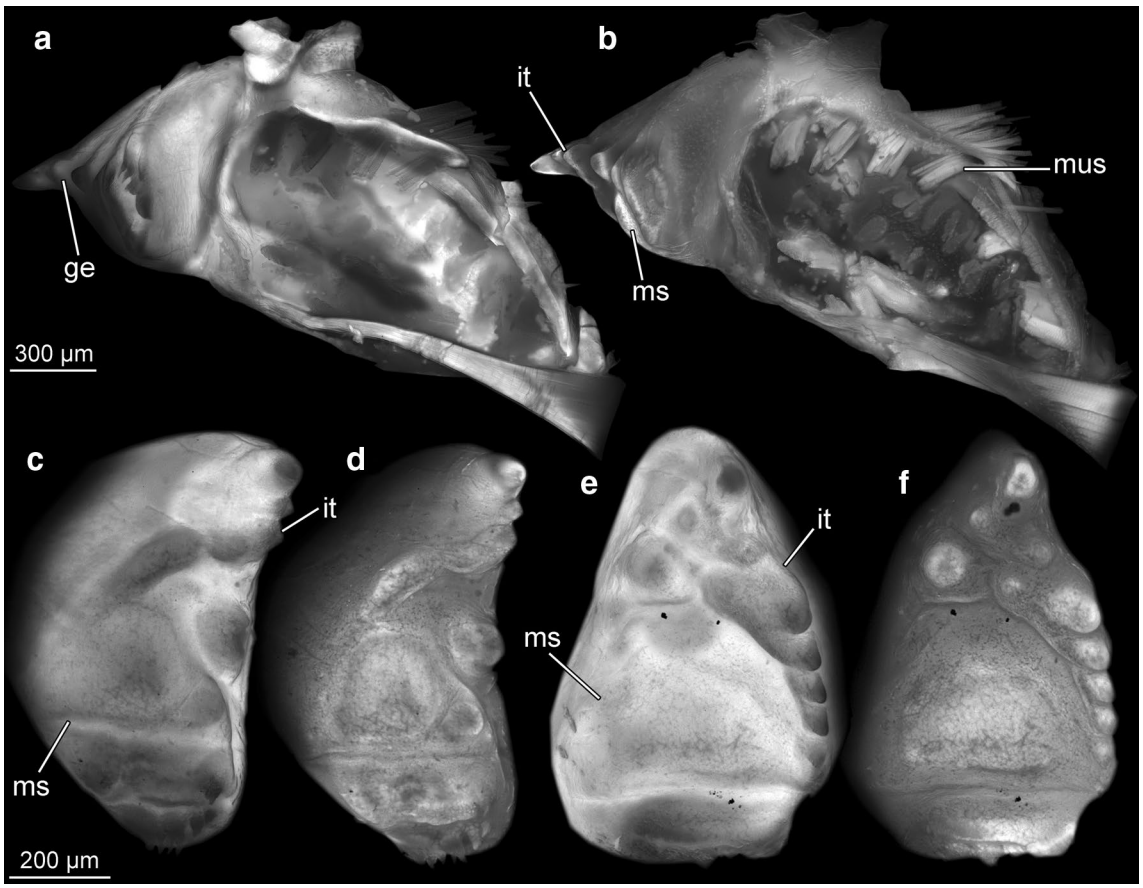

Fig. 12 Isolated mandibles of specimen A. Autofluorescence images (A, C, E. 358 nm; B, D, F. 470 nm). **a**, **b** Proximal view of left mandible. **c**–**f** Median view. **c**, **d** Right mandible. **e**, **f** Left mandible. *ge* gnathal edge, *it* incisive teeth, *ms* molar surface, *mus* muscle

Appendage of post-ocular segment 11 (thoracopod 6): Weakly differentiated into 5 elements; 4 distal elements can be identified as ischium + merus, carpus, fixed finger (propodus) and moveable finger (dactylus); exact identity of 2 proximal elements unclear (Fig. 15a, b, h, i). Slightly longer than preceding appendage. Next layer of cuticle not visible. Appendage tube-shaped; about the same size as preceding appendage. Insertion area of the appendage located further dorsally than preceding appendage. Fluorescence capacities different from maxillipeds (weaker). No setae present. Basipod not clearly distinguishable.

Endopod arising medio-distally from the basipod; tube-shaped; consists of 4 elements. Endopod element 1 not (yet) differentiated into ischium and merus, although future subdivision indicated; longer than wide, about 4×. Endopod element 2 (carpus) longer than wide, about 2×; about half the length of preceding element. Endopod element 3 (propodus) more than 4× longer than wide; about 1.6× longer than preceding element. Endopod element 4 (dactylus) spine-like; longer than wide, about 7×; about the same length of preceding element.

Appendage of post-ocular segment 12 (thoracopod 7): Weakly differentiated into 5 elements; 3 distal elements can be identified as carpus, fixed finger (propodus) and moveable finger (dactylus); exact identity of 2 proximal elements unclear (Fig. 15a, b, j, k). Slightly shorter than preceding appendage. Next layer of cuticle not visible.

Appendage tube-shaped. Insertion area of the appendage located further dorsally than preceding appendage. Fluorescence capacities different from maxillipeds (weaker). No setae present.

Basipod not clearly distinguishable. Endopod arising medio-distally from the basipod; tube-shaped; consists of 4 elements. Endopod element 1 not (yet) differentiated into ischium and merus, although future subdivision indicated; longer than wide, about 3×. Endopod element 2 (carpus) slightly longer than wide; about half the length of preceding element. Endopod element 3 (propodus) curved; longer than wide, about 3×; longer than preceding element, about 1.8×. Endopod element 4 (dactylus) spine-like; longer than wide, about 5×; slightly shorter than preceding element.

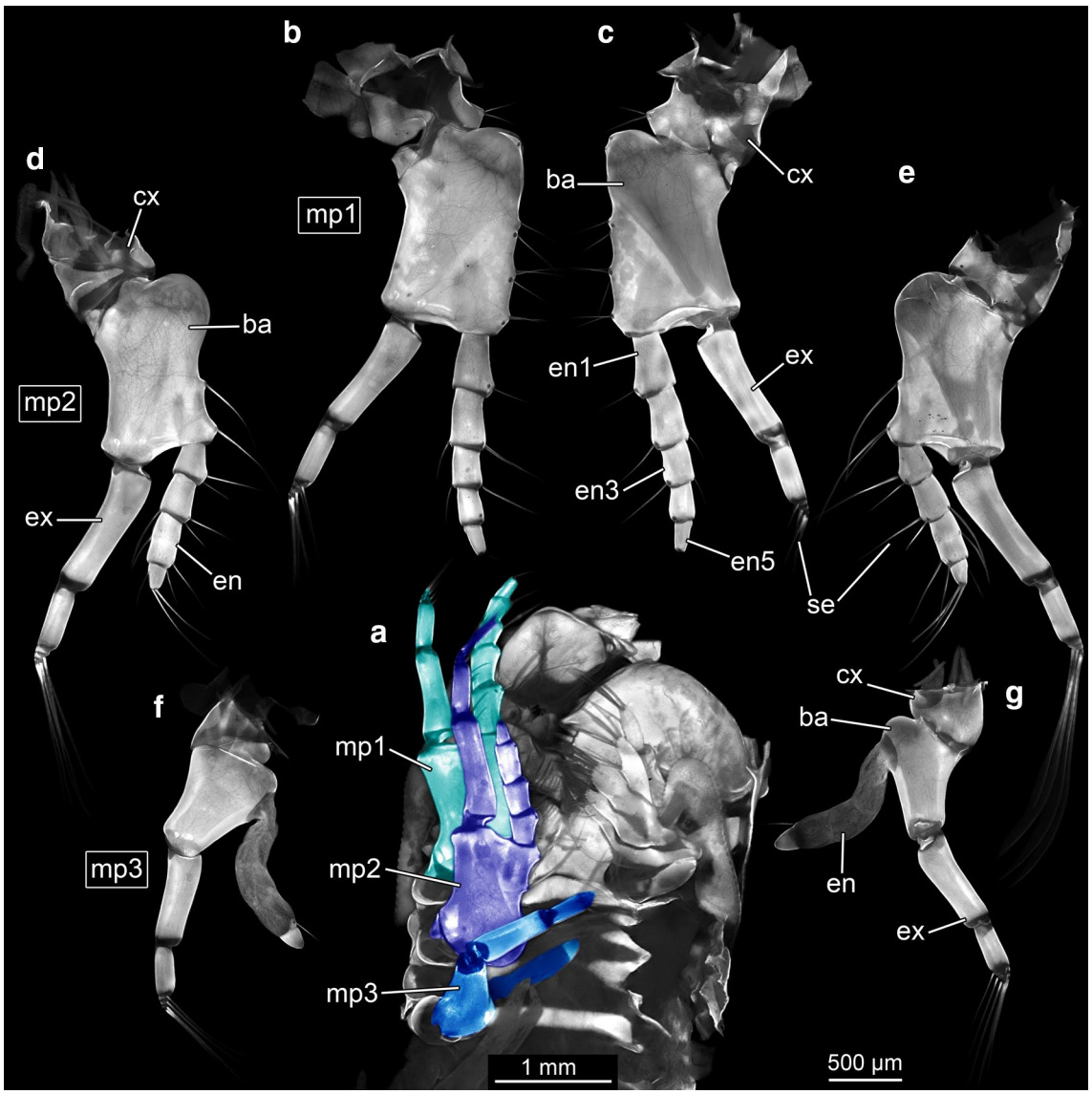

Fig. 13 Maxillipeds of specimen A. Autofluorescence images (358 nm). **a** Colour-marked overview of maxillipeds in situ in ventral view: maxilliped 1 (cyan), maxilliped 2 (violet), maxilliped 3 (blue). **b**–**g** Isolated left maxillipeds. **b**, **d**, **f** Posterior view. **c**, **e**, **g** Anterior view. **b**, **c** Maxilliped 1. **d**, **e** Maxilliped 2. **f**, **g** Maxilliped 3. *Ba* basipod, *cx* coxa, *en* endopod, *en 1–5* endopod element 1–5, *ex* exopod, *mp1–3* maxilliped 1–3, *se* setae

Appendage of post-ocular segment 13 (thoracopod 8): Not (yet) differentiated into discrete elements tube-shaped, curved; embryonic in appearance; about the same size as preceding appendage (Fig. 15a, b, l, m). Fluorescence capacities different from maxillipeds (weaker). No setae present. Insertion area of the appendage not accessible. Next layer of cuticle not visible.

Details of gills (close to thoracopod insertions) Not accessible.

Appendage of post-ocular segment 14 (pleopod 1) Not accessible.

Appendage of post-ocular segment 15 (pleopod 2) Weakly differentiated into basipod, endopod and exopod; no distinct joints visible (yet) (Fig. 16c–f). Next layer of cuticle not visible. Basipod elongated, tube-shaped; longer than wide, about 3.5. Endopod tube-shaped; longer than wide, about 3×. Exopod tube-shaped; longer than wide, more than 2×; longer than exopod, about 2.5×. Appendage with fluorescence capacities different from maxillipeds (weaker). No setae present.

Appendage of post-ocular segment 16 (pleopod 3): Appendage weakly differentiated into basipod, endopod

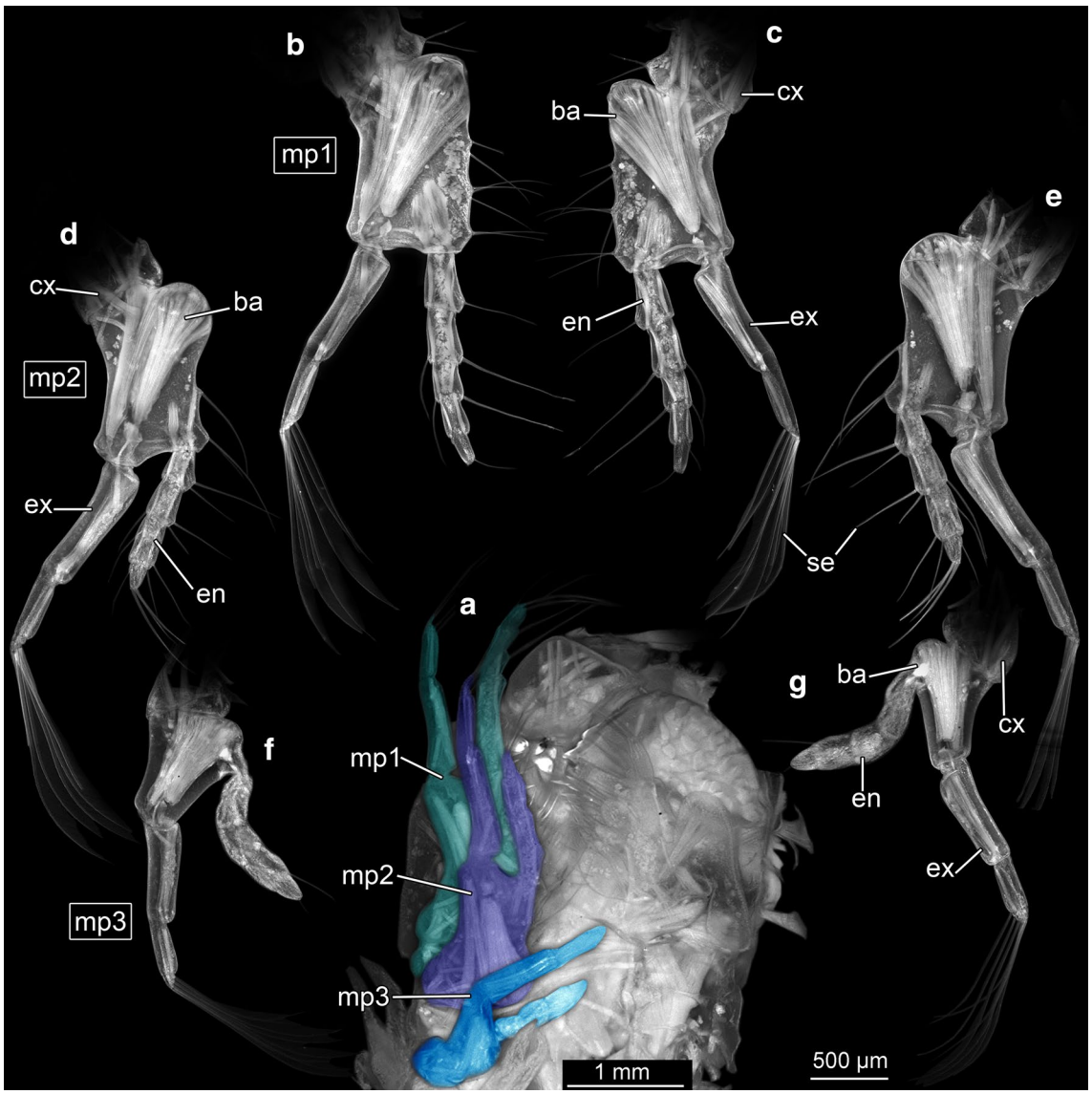

Fig. 14 Maxillipeds of specimen A. Autofluorescence images (470 nm). **a** Colour-marked overview of maxillipeds in situ in ventral view: maxilliped 1 (cyan), maxilliped 2 (violet), maxilliped 3 (blue). **b**–**g** Isolated left maxillipeds. **b**, **d**, **f** Posterior view. **c**, **e**, **g** Anterior view. **b**, **c** Maxilliped 1. **d**, **e** Maxilliped 2. **f**, **g** Maxilliped 3. *ba* basipod, *cx* coxa, *en* endopod, *ex* exopod, *mp1–3* maxilliped 1–3, *se* setae

and exopod; slightly smaller than preceding appendage (Fig. 16b–f). Next layer of cuticle not visible. Basipod elongated, tube-shaped; longer than wide, about 5×.

Endopod tube-shaped; longer than wide, about 3×. Exopod tube-shaped; longer than wide, about 2×; longer than endopod, about 2.5×. Appendage with fluorescence capacities different from maxillipeds (weaker). No setae present.

Appendage of post-ocular segment 17 (pleopod 4): Weakly differentiated into basipod, endopod, and exopod; about the same size as preceding appendage (Fig. 16c–f). Next layer of cuticle not visible. Basipod tube-shaped; longer than wide, about 4×.

Endopod tube-shaped; longer than wide, about 1.8×. Exopod tube-shaped; longer than wide, about 2.4×; longer than endopod, more than 4×. Appendage with fluorescence capacities different from maxillipeds (weaker). No setae present.

Appendage of post-ocular segment 18 (pleopod 5): Weakly differentiated into basipod, endopod and exopod; slightly larger than preceding appendage (16e, f).

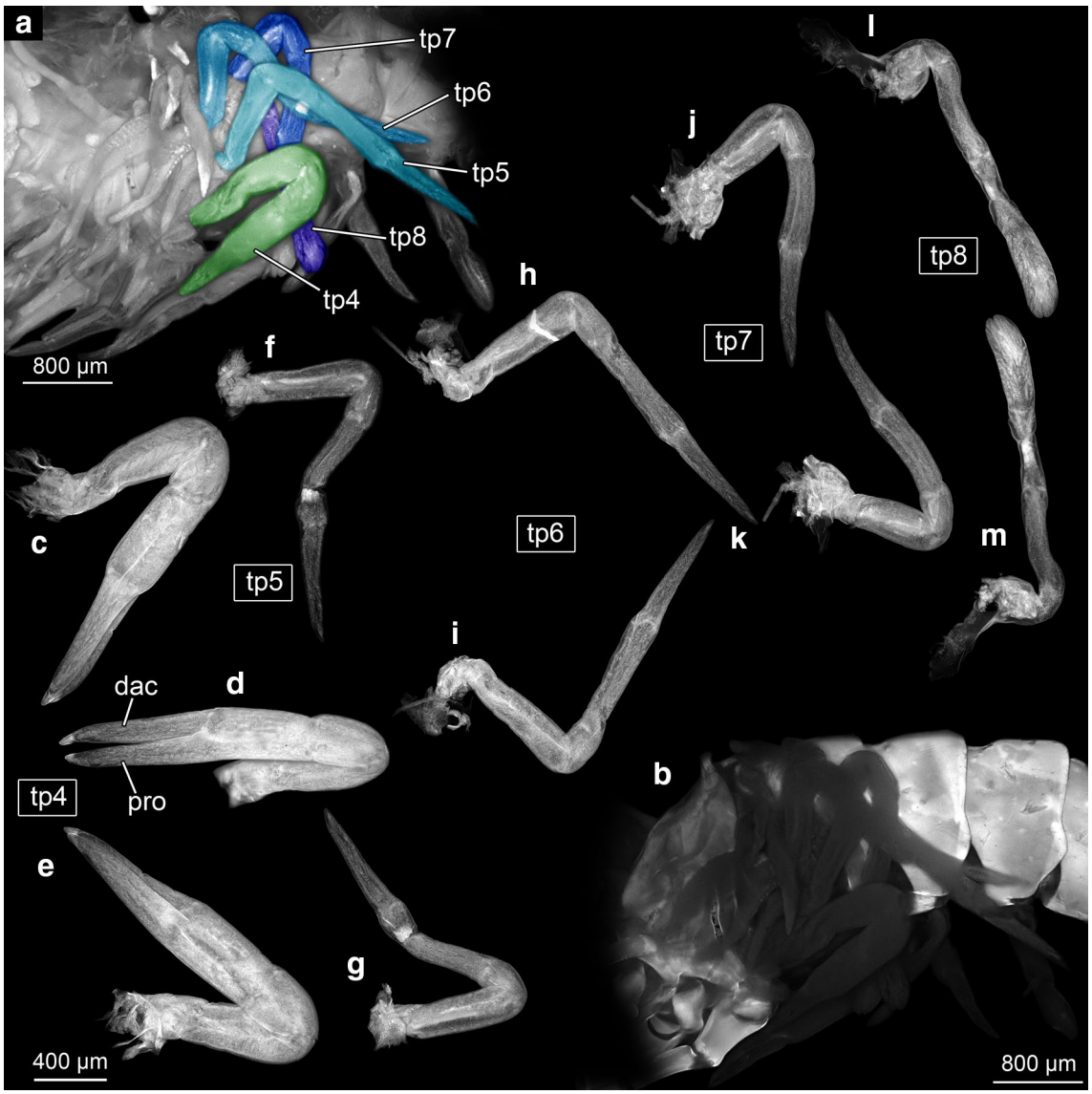

Fig. 15 Thoracopods of specimen A. Autofluorescence images (**a** 470 nm, **b**–**m** 358 nm). A. Colour-marked overview of thoracopods in situ in lateral view: thoracopod 4 (green), thoracopod 5 (cyan), thoracopod 6 (cyan-blue), thoracopod 7 (blue), thoracopod 8 (violet). **b** As A, but without colour-markings. **c**–**m** Isolated left thoracopods. **c**, **f**, **h**, **j**, **l** Anterior view. **d** Lateral view. **e**, **g**, **i**, **k**, **m** Posterior view. **c**–**e** Thoracopod 4. **f**, **g** Thoracopod 5. **h**, **i** Thoracopod 6. **j**, **k** Thoracopod 7. **l**, **m** Thoracopod 8. *dac* dactylus, *pro* propodus, *tp 4–8* thoracopod 4–8

Next layer of cuticle not visible. Basipod tube-shaped; longer than wide, about 4×.

Endopod tube-shaped; longer than wide, about 2×. Exopod tube-shaped; longer than wide, more than 2×; longer than endopod, about 4×. Appendage with fluorescence capacities different from maxillipeds (weaker). No setae present.

Appendage of 19th post-ocular segment (uropod): Generally differentiated into basipod, endopod, and exopod (Fig. 16a–d). Basipod more or less trapezoidal in anterior–posterior view; about as long as wide. Endopod blade-like; with left–right-asymmetry; left endopod longer than wide, about 3.5×, right endopod longer than wide, about 2.5×; with about 20 setae medio-distally. Exopod more or less paddle-shaped; with left–right-asymmetry; left exopod longer than wide, about 3.5×, right exopod longer than wide, about 2.5×. Left exopod longer than left endopod, about 1.8× also wider, about 1.6×; with about 26 setae medio-distally. Surface with (sensorial?) setae.

Gizzard (epidermal anterior part of gut): Sack-like structure with sclerotization on the left and right side,

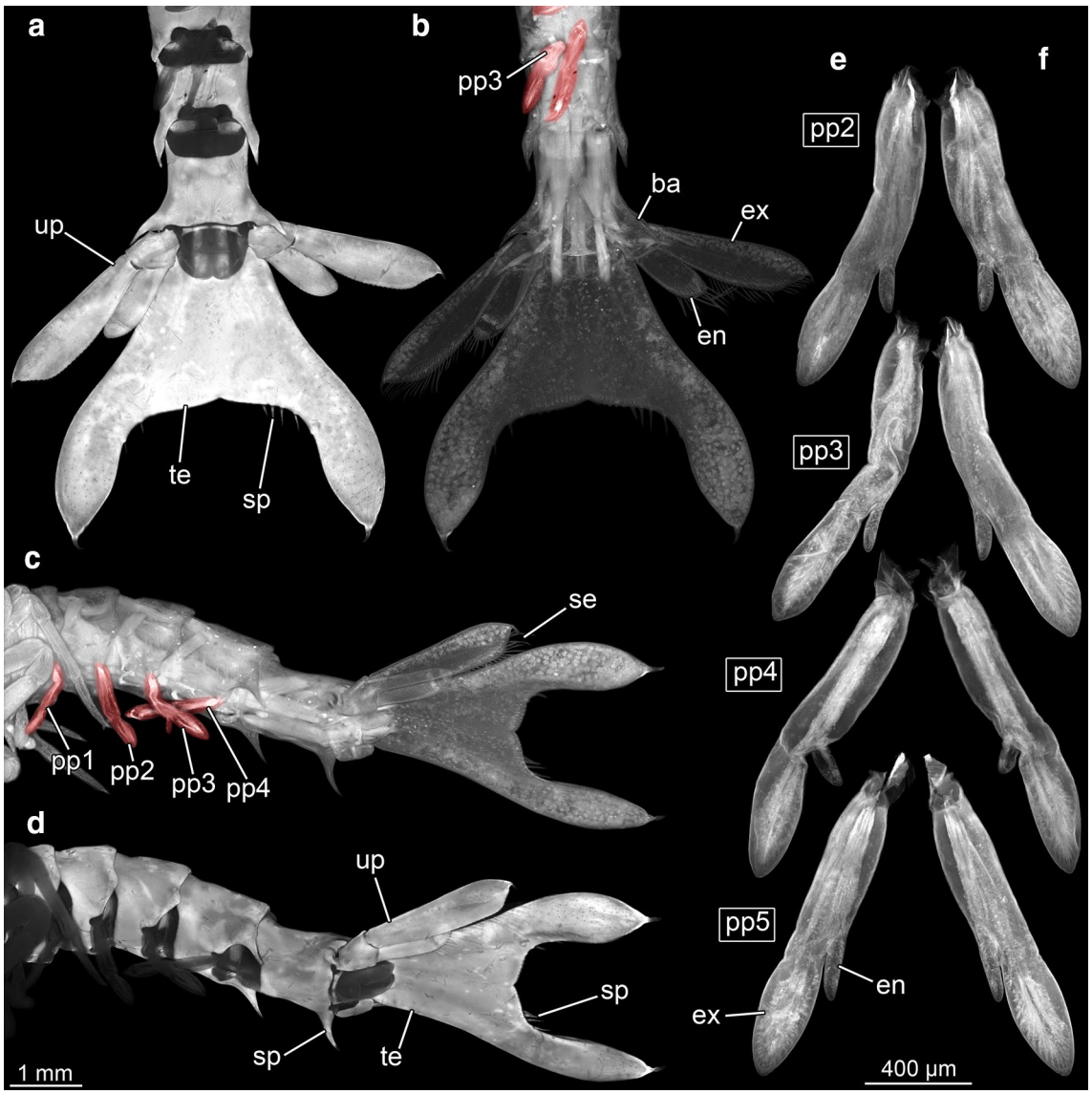

Fig. 16 Pleon and telson of specimen A. Autofluorescence images (**a**, **d**–**f** 358 nm; **b**, **c** 470 nm). **a**, **b** Overview of pleon and telson in ventral view. **b** Colour-marked overview; pleopods (red). **c**, **d** Overview of pleomeres and telson in lateral view. **c** Colour-marked overview; pleopods (red). **e**, **f** Isolated left pleopods. **e** Posterior view. **f** Anterior view. *ba* basipod, *en* endopod, *ex* exopod, *pp 2–5* pleopod 2–5, *se* setae, *sp* spines, *te* telson, *up* uropod

probably precursors of teeth; long setae in this area; short setae more in the middle (Fig. 17). Gizzard subdivided into 3 parts. No distinct teeth (yet?). Part 1 (median part) with numerous setae differing in length and width; long setae in the sclerotized part; distal end appears to pass into a Reusen-apparatus with lamellae and probably small teeth or spines. Lamellae not (yet?) sclerotized. Distinct v-shaped sclerotization in the middle; posterior a field with lamellae. Part 2 and 3 (sidebar 1 and 2) with long setae in this area and short setae more in the middle.

Description of Specimen B

Habitus: Small euarthropodan larva with strongly elongated and arched shield ("carapace") (Figs. 1b, 2b, 3d). Body differentiated into cephalothorax, pleon, and non-somitic telson and organised into 20 segments: ocular segment plus 19 appendage-bearing (post-ocular) segments. Ocular segment incorporated into the cephalothorax, the dorsal area contributes to the shield. Post-ocular segments 1 to 13 incorporated into the cephalothorax, their dorsal areas contribute to the shield.

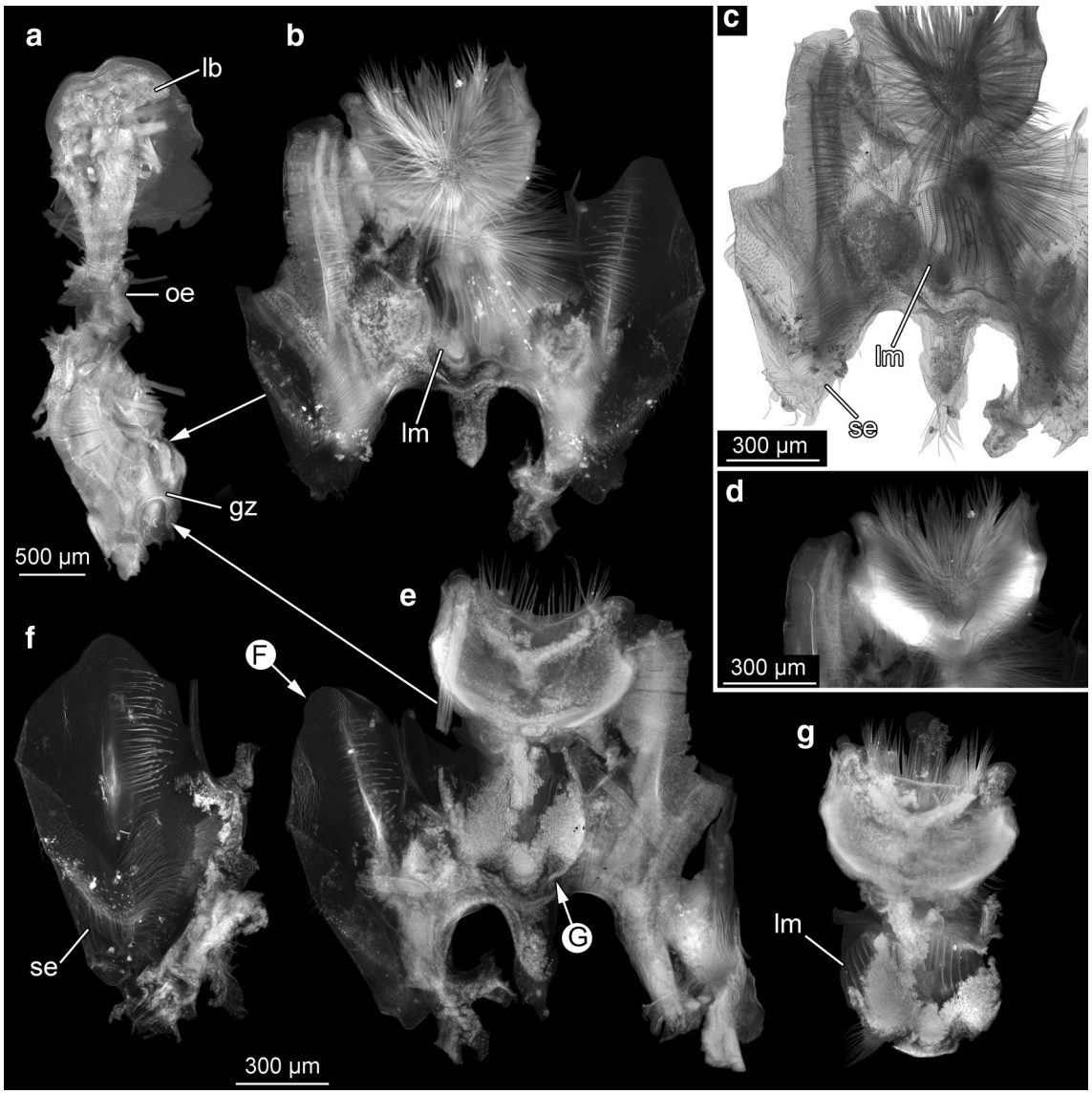

Fig. 17 Gizzard of specimen A. Autofluorescence images (**a**, **b**, **e**–**g** 470 nm, **d** 358 nm) besides **c** which was recorded under transmitted white light conditions. **a** Overview of gizzard and labrum. **b**–**g** Opened gizzard. **b**–**d** Inner view of gizzard. **b**, **c** Overview. **d** Close-up of sclerotic arch. **e**–**g** Outer view of gizzard. **e** Overview. **f** Isolated part 1. **g** Isolated part 2. *gz* gizzard, *lb* labrum, *lm* lamellae, *oe* oesophagus, *se* setae

Post-ocular segments 14 to 19 are all separate pleon segments, each dorsally forming a tergite.

Cephalothorax: Shield in dorsal view large and prominent and occupying 6/7 of the total length of the larva (observing overall length including all protruding structures). Anterior rim of the shield drawn out into a very prominent, rostrum (Fig. 18a, b). Rostrum elongated triangular shaped; occupying about ½ of the total length of the larva; longer than wide, about 5×. About 10 spines on each side of the lateral rim; with two distinct structures: a trapezoidal field with 4 distinct pores; positioned after about 1/7 of the rostrum length (Fig. 18c, e, f) and a median trapezoidal muscle attachment depression (Fig. 18a, d).

Main part of shield more or less trapezoidal in dorsal view, longer than wide, about 1.4×, with a flat v-shaped notch at the posterior rim. A cleft in the middle of the posterior rim continues into a keel almost reaching the muscle attachment structures; more or less rectangular in dorsal view, about as long as wide, with a rounded notch at the posterior rim; no keel visible.

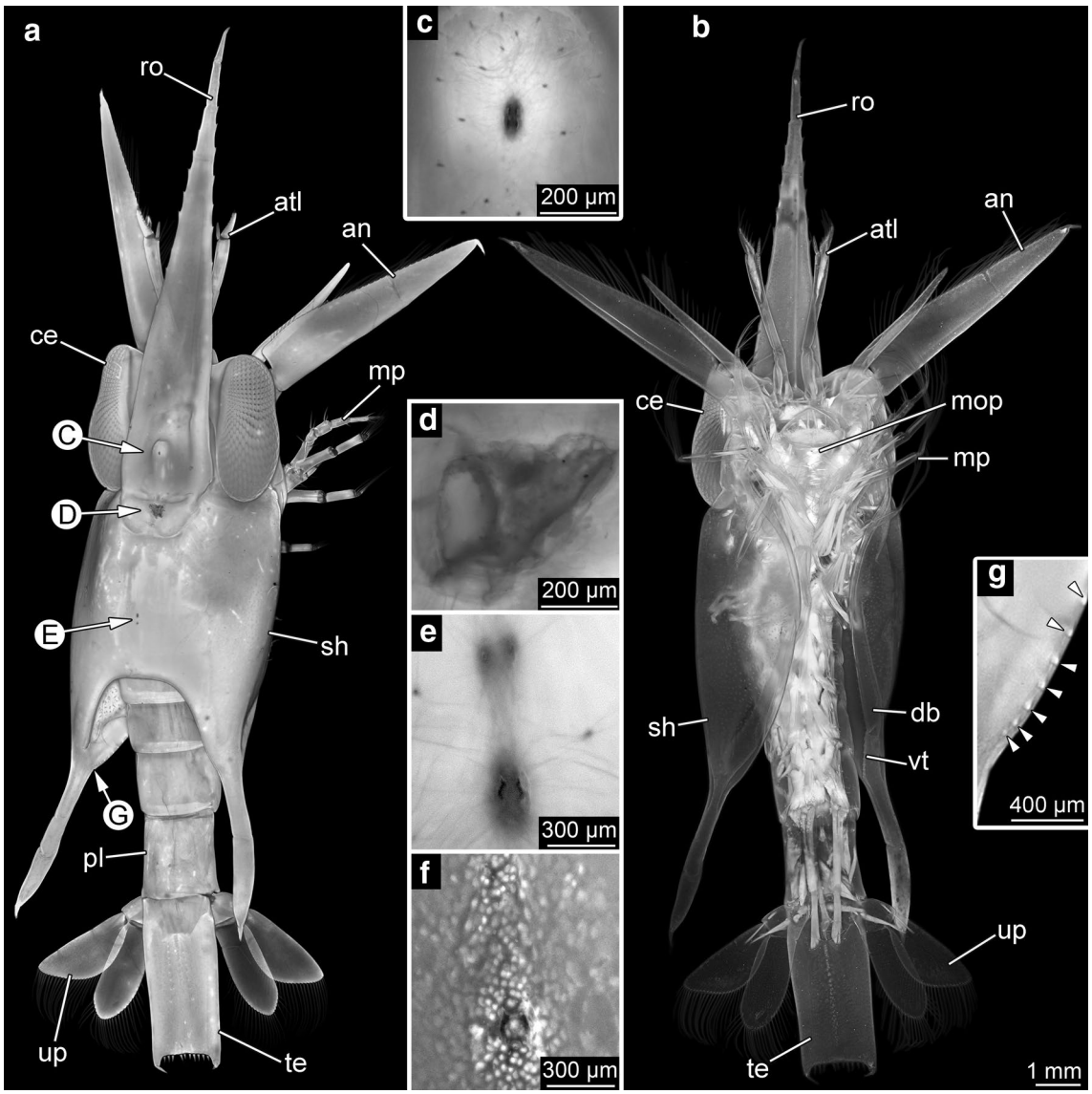

Fig. 18 Overview images and details of eyes and shield of specimen B, autofluorescence images (**a**, **c**, **d**, **e**, **g**. 358 nm, **b**, **f** 470 nm). **a** Overview in dorsal view. **b** Overview in ventral view. **c** Close-up on possible sensory dorsal organ of rostrum. **d** Close-up on muscle attachments of mandibles positioned on the rostrum. **e**, **f** Close-up on possible sensory dorsal organ of shield. **g** Close-up on ventral teeth. *an* antenna, *atl* antennula, *ce* compound eye, *db* doublure, *mop* mouthparts, *mp* maxillipeds, *pl* pleon, *ro* rostrum, *sh* shield, *te* telson, *vt* ventral teeth, *up* uropods

Postero-lateral edges drawn out into 2 long spines; longer than wide, about 3.4× and longer than main part of the shield, about 1.3×.

Surface of shield without any ridges or keels. Ventro-lateral edges of shield with a doublure elongating into the spines. Ventral edge with small teeth. Dorsal surface of shield with a circular field positioned in the middle of the posterior part of the shield; consisting of 2 pores posterior of the circular field.

Overall surface of shield with some (possibly sensorial) setae in dorsal view; not accessible in ventral view.

Pleon: (Fig. 2b, 18a, b) Tergite of post-ocular segment 14 (pleomere 1) not fully accessible.

With one spine on each lateral side (possible precursor structures of the tergopleura); Postero-lateral edges with tergite continuous to the ventral sclerotisation (sternite).

Tergite of post-ocular segment 15 (pleomere 2) rectangular in dorsal view; wider than long, about 2×. With one spine on each lateral side (possible precursor structures of the tergopleura). Postero-lateral edges of tergite continuous with the ventral sclerotisation (sternite).

Tergite of post-ocular segment 16 (pleomere 3) rectangular in dorsal view; wider than long, about 2×; slightly longer and slightly narrower than preceding segment. With one spine on each lateral side (possible precursor structures of the tergopleura). Postero-lateral edges of tergite continuous with the ventral sclerotisation (sternite).

Tergite of post-ocular segment 17 (pleomere 4) rectangular in dorsal view; wider than long, about 1.5×; longer and than preceding segment, about 1.3×, also slightly narrower. With one spine on each lateral side (possible precursor structures of the tergopleura). Postero-lateral edges of tergite continuous with the ventral sclerotisation (sternite).

Tergite of post-ocular segment 18 (pleomere 5) rectangular in anterior–posterior view; about as wide as long; longer and than preceding segment, about 1.3×, also slightly narrower. With one spine on each lateral side (possible precursor structures of the tergopleura). Postero-lateral edges of tergite continuous with the ventral sclerotisation (sternite).

Tergite of post-ocular segment 19 (pleomere 6) square-shaped; slightly longer and less wide than preceding appendage. With one spine on each lateral side (possible precursor structures of the tergopleura). Postero-lateral edges of tergite continuous with the ventral sclerotisation (sternite).

Surface with some setae in dorsal view; not accessible in ventral view.

Telson: Elongated rectangular in dorsal view, slightly concave posterior rim; with one spine as extension of the lateral rim on each side; longer than wide, more than 2× (Figs. 1b, 2b). Posterior rim bearing 10 spine-like setae; all about the same size (Fig. 6a, b). The anal opening not visible. Surface with few setae forming about 3 distinct rows from anterior to posterior; not accessible in ventral view.

Ocular segment Bearing a pair of compound eyes, each one inserting laterally (Fig. 18a, b). Each compound eye is differentiated into proximal stalk and distal cornea. Corneal region with distinct facets, indicating ommatidia. Length of compound eye about 1/7 of the total length of the larva. Compound eye in dorsal view more or less bean-shaped; with an inward curvature at the lateral side; longer than wide only, about 2.5×, considering only the ommatidia region. Without a chromatophore on the base (Fig. 19a, b).

Compound eye in lateral view more or less bean-shaped, appears to be a rounded rectangular structure in anterior–posterior view; longer than wide, about 2.5× (Figs. 8, 19c). In anterior view oval with trapezoidal stalk in anterior–posterior view. In posterior view circular in outline. Ommatidia arranged in 26 ommatidia rows from anterior to posterior (rows strongly curving anteriorly and posteriorly). Ommatidia rows with about 20 ommatidia in each row in the middle; anterior and posterior fewer ommatidia per row. Facet shape hexagonal, squared or intermediate; an area with squared ommatidia antero-dorsally positioned in row 6 to 11; around this area facets of intermediate shape (Figs. 7b, 19b).

Hypostome-labrum complex with triangular labrum (ventral view) with the tip pointing towards the anterior part; wider than long, exact dimensions not accessible.

Appendage of post-ocular segment 1 (antennula) Generally differentiated into peduncle and 2 flagella; about half the size of the rostrum (Fig. 20a–c). Peduncle tube-shaped and not (yet) subdivided into separate elements; future subdivision into 3 elements indicated by folds; longer than wide, about 7×; with 1 seta medio-distally. Flagellum 1 (median) spine-like and not (yet) subdivided into ringlets. Flagellum 2 (lateral) more or less triangular in anterior–posterior view; larger than flagellum 1, about 2×; not (yet) subdivided into ringlets; with 13 setae medially.

Appendage of post-ocular segment 2 (antenna) Generally differentiated into coxa, basipod, endopod and exopod (Fig. 20a, d, e). Antenna longer than preceding appendage, about 1.8×.

Coxa trapezoidal in anterior–posterior view; longer than wide, about 1.5×. No setae present. Basipod more or less trapezoidal in anterior–posterior view; slightly longer than wide. Medio-lateral edge drawn out into a small spine. Postero-distal edge drawn out into a prominent spine. Proximo-lateral edge bearing one tube-shaped apophysis. Endopod arising medio-distally from the basipod; tube-shaped, tapering distally; slightly smaller than entire antennula. No setae present. Exopod arising latero-distally from the basipod; more or less tube-shaped, consisting of 1 element and a spine distally; multiple setae medially; longer than endopod, about 2×, also wider about, 3×. Surface with few setae in dorsal and ventral view.

Appendage of post-ocular segment 3 (mandible) Generally differentiated into coxa with endite and mandibular palp (Fig. 21a, b, d). Coxa medially forming gnathal edge, differentiated into pars molaris with 2 teeth and pars incisivus with 5 teeth. Teeth of the left mandible not accessible.

Mandibular palp minute, lobe-like, not further differentiated. Sternal protrusion of mandibular segment (paragnaths) more or less rounded triangular in anterior–posterior view, lobe-like with massive base; longer than wide, about 2×. Entire surface covered with small short setae.

Appendage of post-ocular segment 4 (maxillula) Generally differentiated into coxa, basipod, and endopod;

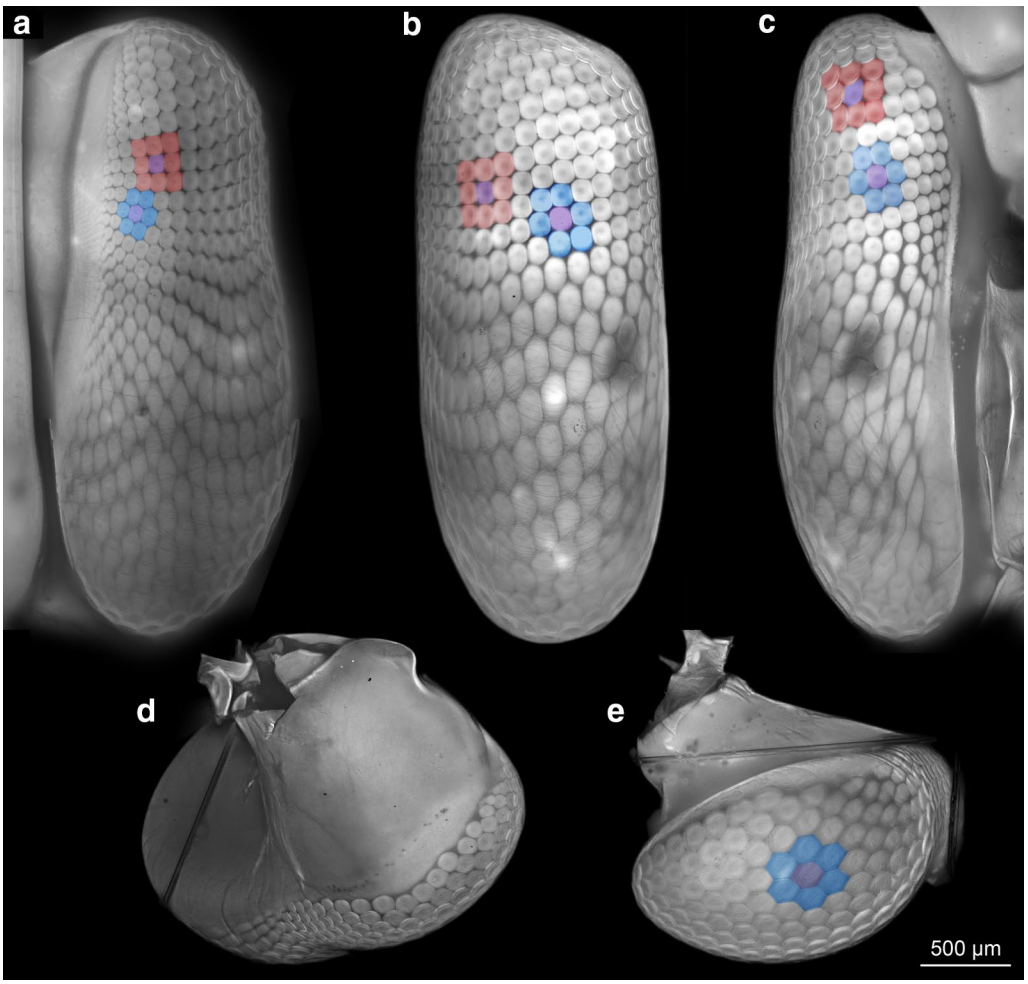

Fig. 19 Autofluorescence images (358 nm) of eyes of specimen B; note different shapes of facets: ommatidium (purple) surrounded by eight ommatidia (red) = squared arrangement; ommatidium (purple) surrounded by six ommatidia (blue) = hexagonal arrangement. **a**–**c** Colour-marked left eye. **d**, **e** Colour-marked right eye. **a** Dorsal view. **b** Lateral view. **c** Ventral view. **d** Posterior view. **e** Anterior view

slightly smaller than preceding appendage (Fig. 21a, b, f). Coxa medially drawn out into coxal endite; laterally forming distinct sclerite. Coxal endite paddle-shaped, curved, with about 9 setae distally. Wider than basipodal endite, about 4×; with 16 setae distally. Basipod trapezoidal in anterior–posterior view, medially drawn out into distinct endite; longer than wide, about 2.4×. Basipodal endite blade-like; wider than coxal, 1.6×; with 13 setae distally. Endopod arising medio-distally from the basipod; tube-shaped; about half as long as the coxal endite; with 3 setae distally.

Appendage of post-ocular segment 5 (maxilla) Generally differentiated into coxa, basipod, endopod and exopod; about as large as preceding appendage (Fig. 21a, i). Coxa medially with 2 endites: Proximal coxal endite blade-shaped; with about 14 setulose setae; 10 setae evenly distributed along the median edge; 4 setae arising from the posterior surface of the endite; all pointing medially. Distal coxal endite tube-like, smaller than proximal coxal endite; with 3 setulose setae; 1 seta on the median edge; 1 seta arising from the posterior surface of the endite; 1 seta on the side towards the proximal basipodal endite; all pointing medially.

Basipod medially with 2 endites: Proximal basipodal endite with about 13 setulose setae; 12 setae evenly distributed along the median edge; 1 seta on the side towards the distal basipodal endite; all pointing medially. Distal basipodal endite blade-like; slightly larger than proximal basipodal endite; about the same size as proximal coxal endite; with about 13 setae, some of them setulose; 12 setae evenly distributed along the median edge; 1 seta arising from the posterior surface of the endite; all pointing medially.

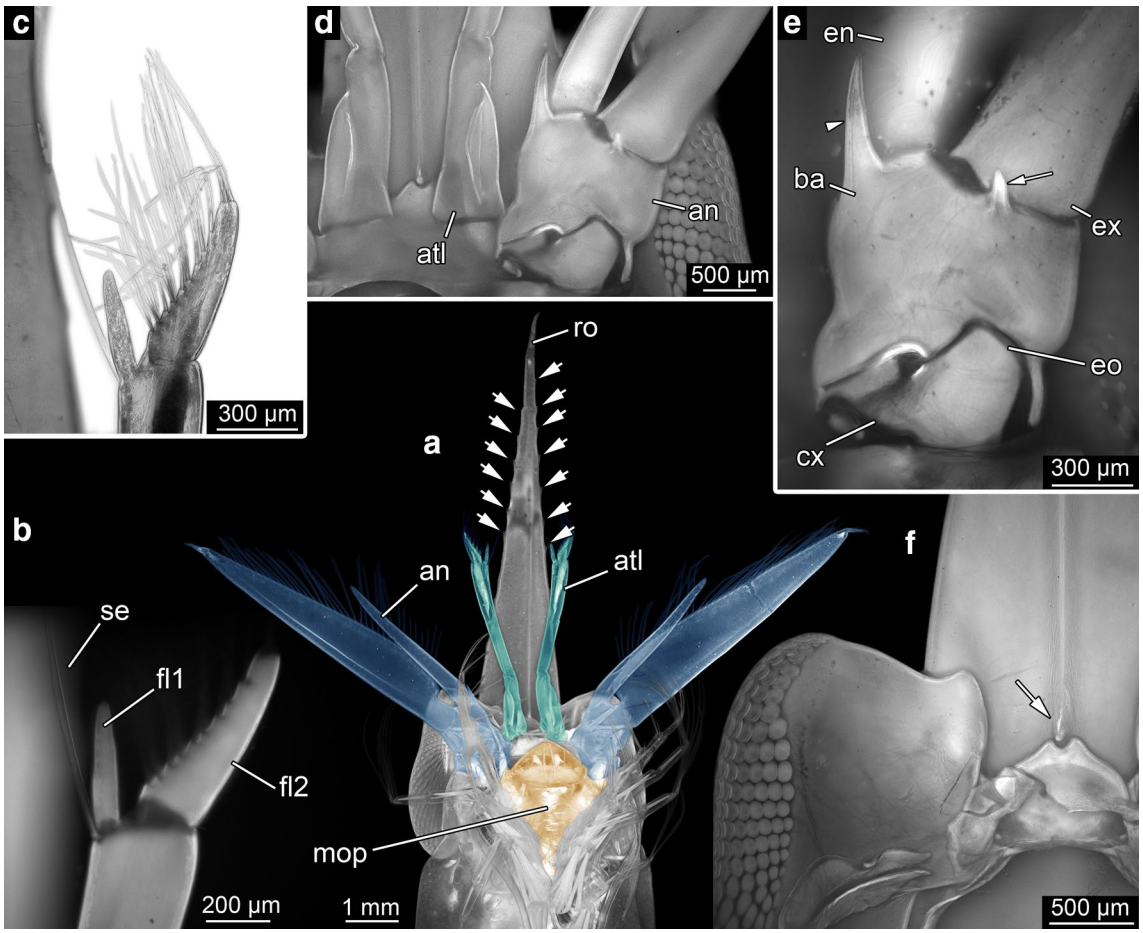

Fig. 20 Anterior body area of specimen B, ventral view. Composite autofluorescence images (358 nm) besides C, which was recorded under transmitted white light conditions. **a** Colour-marked overview, antennula (cyan), antenna (blue) and mouthparts (orange); note the spines on the rostrum (arrows). **b**, **c** Close-up on flagella and setae of left antennula. **d** Close-up on coxa and basipod of left antenna and on proximal area of peduncle of antennulae. **e** Close-up on proximal region of left antenna; note large spine (arrowhead) and small spine (arrow). **f** Close-up on part of eye and proximal area of rostrum; note the spine-like structure (arrow). *an* antenna, *atl* antennula, *ba* basipod, *cx* coxa, *en* endopod, *eo* excretory organ, *ex* exopod, *fl1, 2* flagellum 1, 2, *mop* mouthparts, *ro* rostrum, *se* setae

Endopod arising medio-distally from the basipod; tube-shaped; longer than wide, about 4×; with about 6 setae, some of them setulose; 4 setae evenly distributed along the median edge; 2 setae arising from the posterior surface of the endite; all pointing medially (Fig. 22a, b, e).

Exopod arising latero-distally from the basipod; prominent, lobe-like; 2 distinct regions are distinguishable: proximal region paddle-like; proximo-lateral edge of paddle extending into second fin-shaped region oriented towards the main body; with setulose setae around the entire rim and one single prominent seta at the disto-lateral tip of the fin-shaped region (Fig. 22a, c, d).

Appendage of post-ocular segment 6 (maxilliped 1) Generally differentiated into coxa, basipod, endopod and exopod (Fig. 23a–c). Coxa differentiated into median and lateral sclerite. Further details not accessible; medially with 2 setae. Basipod rectangular in anterior–posterior view; longer than wide, about 2×; medially with 8 setae arranged in 4 groups, 1 group far proximally, 3 groups further distally.

Endopod arising medio-distally from the basipod; consists of 5 tube-shaped elements; medially with 11 setae arranged in 4 groups, 1 group far proximally, 3 groups further distally. Endopod element 1 (ischium) longer than wide, about 3×; medio-distally with about 7 setae arranged in 2 groups. Endopod element 2 (merus) more complex in shape, Fig. 7-shaped in anterior–posterior view; with about 3 setae medio-distally and a prominent seta arising laterally pointing towards the body. About as long as wide; almost half as long,

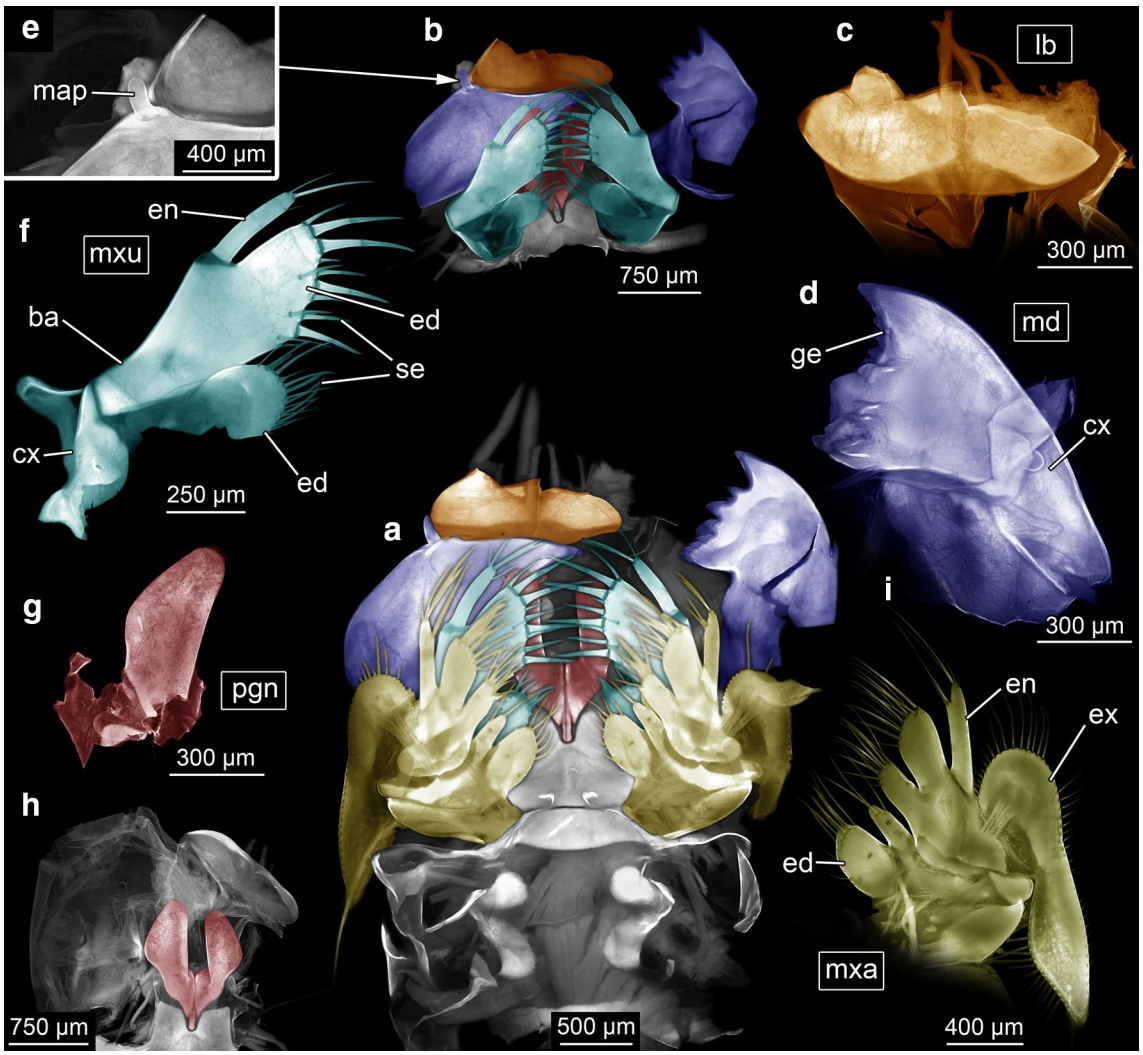

Fig. 21 Mouthparts of specimen B. Autofluorescence images (358 nm). **a** Colour-marked overview of mouthparts in situ in ventral view: labrum (orange), mandibles (violet), paragnaths (red), maxillulae (cyan), and maxillae (yellow). **b** As **a**, but with maxillae removed. **c**–**i** Isolated mouthparts. **c** Labrum. **d** Mandible. **e** Close-up on mandibular palp of mandible. **f** Maxillula. **g** Paragnath. **h** Overview of paragnaths (red). **i** Maxilla. *ba* basipod, *cx* coxa, *ed* endite, *en* endopod, *ex* exopod, *ge* gnathal edge, *lb* labrum, *map* mandibular palp, *md* mandible, *mxa* maxilla, *mxu* maxillula, *pgn* paragnaths, *se* setae

but wider than element 1. Endopod element 3 (carpus) about as long as wide; slightly smaller than element 2; with about 4 setae medio-distally. Endopod element 4 (propodus) longer than wide, about 2×; slightly longer but slightly narrower than element 3; with about 5 setae medio-distally. Endopod element 5 (dactylus) longer than wide, about 2×; half as wide as element 4; with about 9 setae distally.

Exopod arising latero-distally from basipod; tube-shaped; with 2 prominent elements proximally and a distal region subdivided into 3 ringlets; longer than wide, about 6×; ¾ of the length of the endopod; with about 8 setulose setae distally arising from the 3 ringlets.

Appendage of post-ocular segment 7 (maxilliped 2) Generally differentiated into coxa, basipod, endopod and exopod; slightly smaller than preceding appendage (Fig. 23a, d, e). Coxa differentiated into median and lateral sclerite. Further details not accessible. Basipod rectangular in anterior–posterior view; longer than wide, about 2×; medially with 4 setae arranged in 2 groups. Endopod arising medio-distally from the basipod; consists of 5 tube-shaped elements; about half the size of preceding appendage.

Endopod element 1 (ischium) slightly longer than wide; medio-distally with 2 setae arranged in 2 groups. Endopod element 2 (merus) longer than wide, about 1.7×;

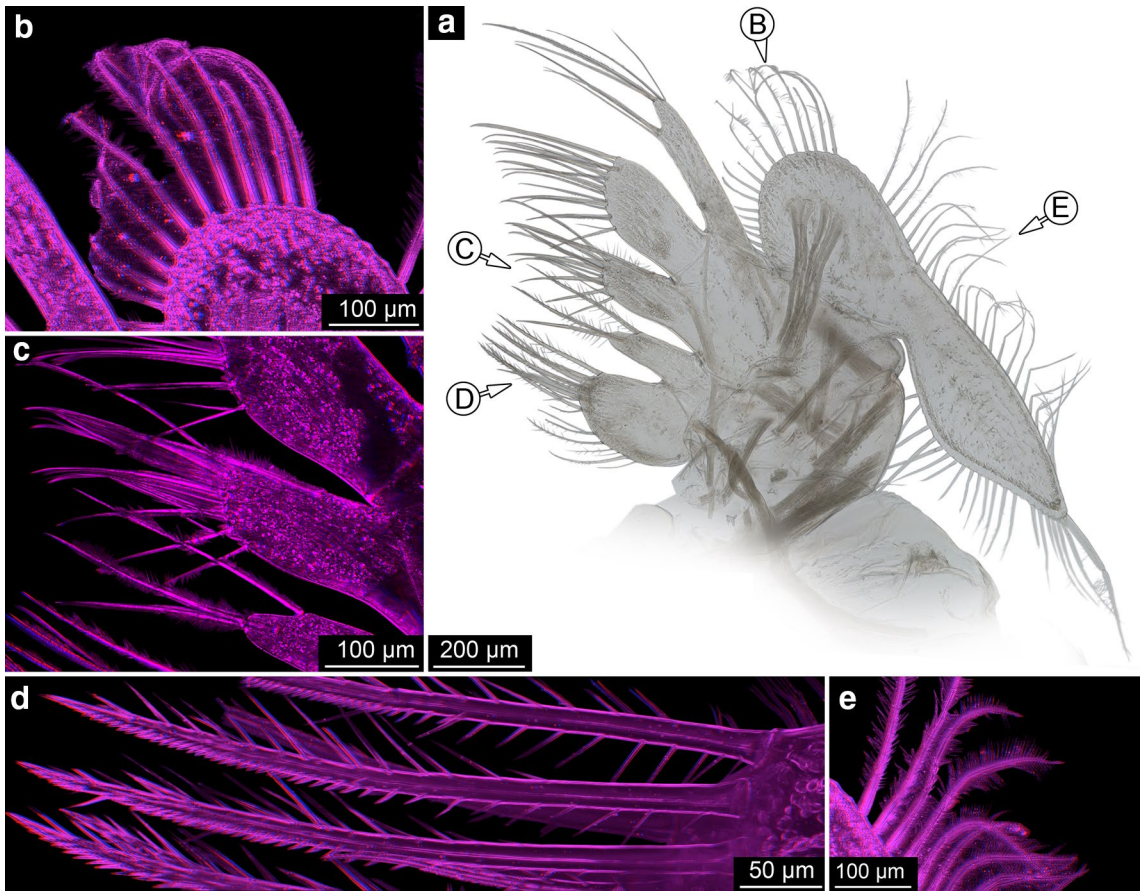

Fig. 22 Posterior overview and details of isolated right maxilla of specimen B. **a** Transmitted white light. **b**–**e** Stereo images derived from image stack recorded under phase contrast (**b**, **c**, **e**) or under white light (**d**). **b**, **e** Close-up on setae and setules of exopod. **c** Close-up on setae and setules of coxal and basipodal endites. **d** Close-up on setae and setules of coxal endite

about as long as element 1; medio-distally with 4 setae arranged in 2 groups and 1 seta latero-distally. Endopod element 3 (carpus) not set off from element 4; about as long as wide; about half the length of element 2. With 1 seta latero-distally. Endopod element 4 (propodus) about as long as wide; about the same size as preceding element; with 2 setae medio-distally and 1 seta latero-distally. Endopod element 5 (dactylus) longer than wide, about 2×; not as wide as element 4; with about 5 setae distally and 1 seta medio-proximally.

Exopod arising latero-distally from the basipod; tube-shaped; longer than wide, about 5×; with 2 prominent elements proximally and a distal region subdivided into 3 ringlets; about ¼ longer than endopod; slightly longer than exopod of appendage 6; with 7 setae distally arising from the 3 ringlets.

Appendage of post-ocular segment 8 (maxilliped 3) Generally differentiated into coxa, basipod, endopod and exopod; about 2/3 of the length and width of preceding appendage (Fig. 23a, f, g). Coxa differentiated into median and lateral sclerite. Further details not accessible. Basipod more or less triangular; almost half as wide as long.

Endopod arising medio-distally from the basipod; tube-shaped; distal part sclerotised, proximal part unsclerotised, soft; longer than wide, about 2×. Exopod arising latero-distally from the basipod; tube-shaped; about 2/3 of the length of exopod of appendage 7; with 2 prominent elements proximally and a distal region subdivided into 3 ringlets; longer than wide, about 4×; longer than endopod, about 2.5×; with about 7 setae distally arising from the 3 ringlets.

Appendage of post-ocular segment 9 (thoracopod 4) Not (yet) differentiated into discrete elements embryonic in appearance; future subdivision indicated (Fig. 24a, b, g). Fingers more than 1/3 of the size of thoracopod. Next layer cuticle visible; distinct gap between outer and inner cuticle. Appendage tube-shaped; fluorescence capacities different from maxillipeds (weaker). No setae present.

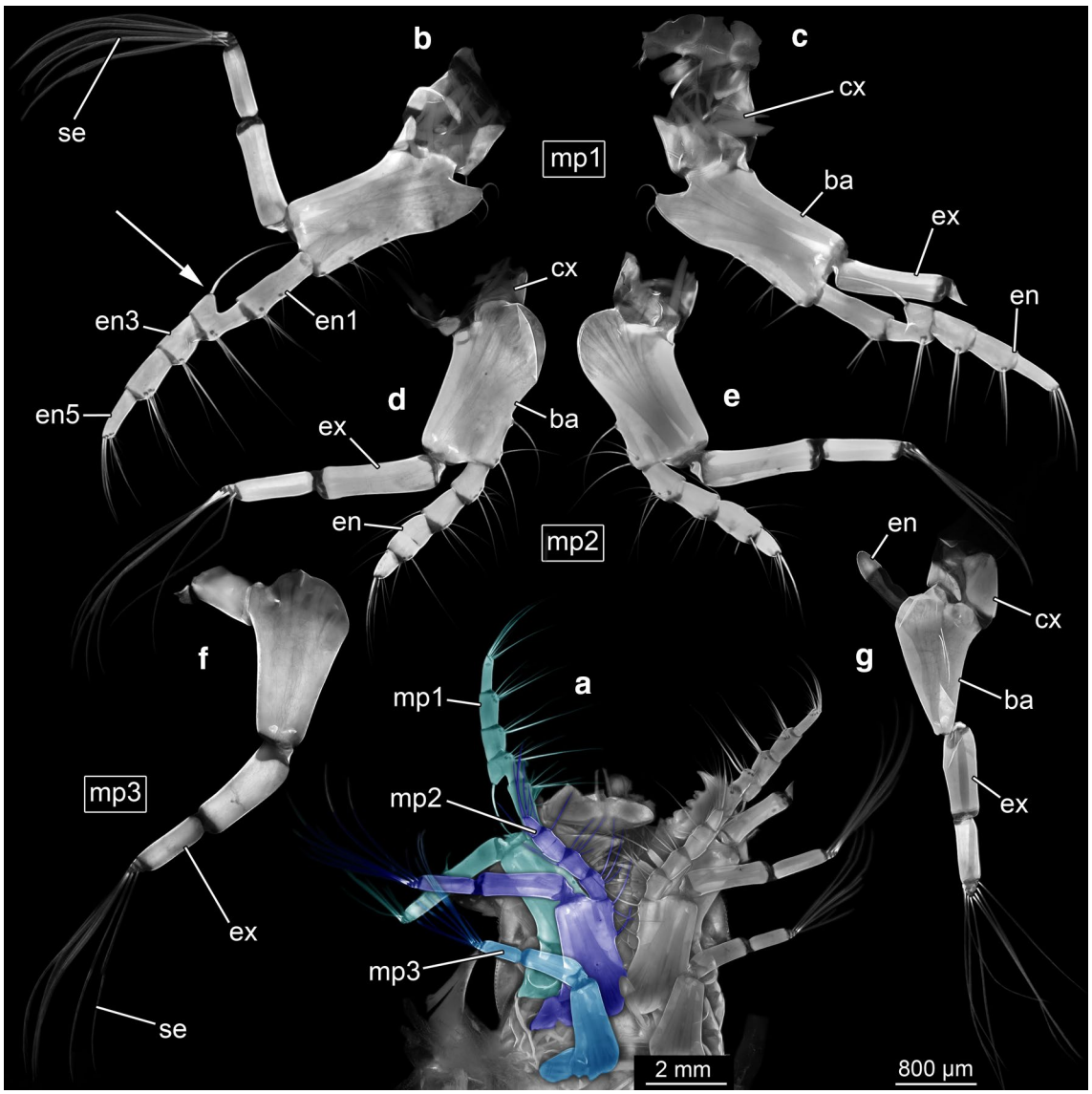

Fig. 23 Maxillipeds of specimen B. Autofluorescence images (358 nm). **a** Colour-marked overview of maxillipeds in situ in ventral view: maxilliped 1 (cyan), maxilliped 2 (violet), maxilliped 3 (blue). **b**–**g** Anterior view of isolated maxillipeds. **b**, **d**, **f** Right maxillipeds. **c**, **e**, **g** Left maxillipeds. **b**, **c** Maxillipeds 1; note the hook-like structure on endopod element 2 (arrow). **d**, **e** Maxillipeds 2. **f**, **g** Maxillipeds 3. *ba* basipod, *cx* coxa, *en* endopod, *en 1–5* endopod element 1–5, *ex* exopod, *mp1–3* maxilliped 1–3, *se* setae

Appendage of post-ocular segment 10 (thoracopod 5) Not (yet) differentiated into discrete elements embryonic in appearance; other structures not (yet) recognizable; distally spine-like; smaller than preceding appendage (Fig. 24a, c, g). Next layer of cuticle visible; distinct gap between outer and inner cuticle. Appendage tube-shaped. Insertion area of the appendage located further dorsally than preceding appendage. Fluorescence capacities different from maxillipeds (weaker). No setae present.

Appendage of post-ocular segment 11 (thoracopod 6) Not (yet) differentiated into discrete elements embryonic in appearance, dactylus as only differentiated structure, other structures not (yet) recognizable; distally spine-like; about the same size as preceding appendage (Fig. 24a, d, g). Next layer of cuticle visible; distinct gap between outer and inner cuticle. Appendage tube-shaped; about the same size as preceding appendage. Insertion area of the appendage located further dorsally than preceding appendage. Fluorescence

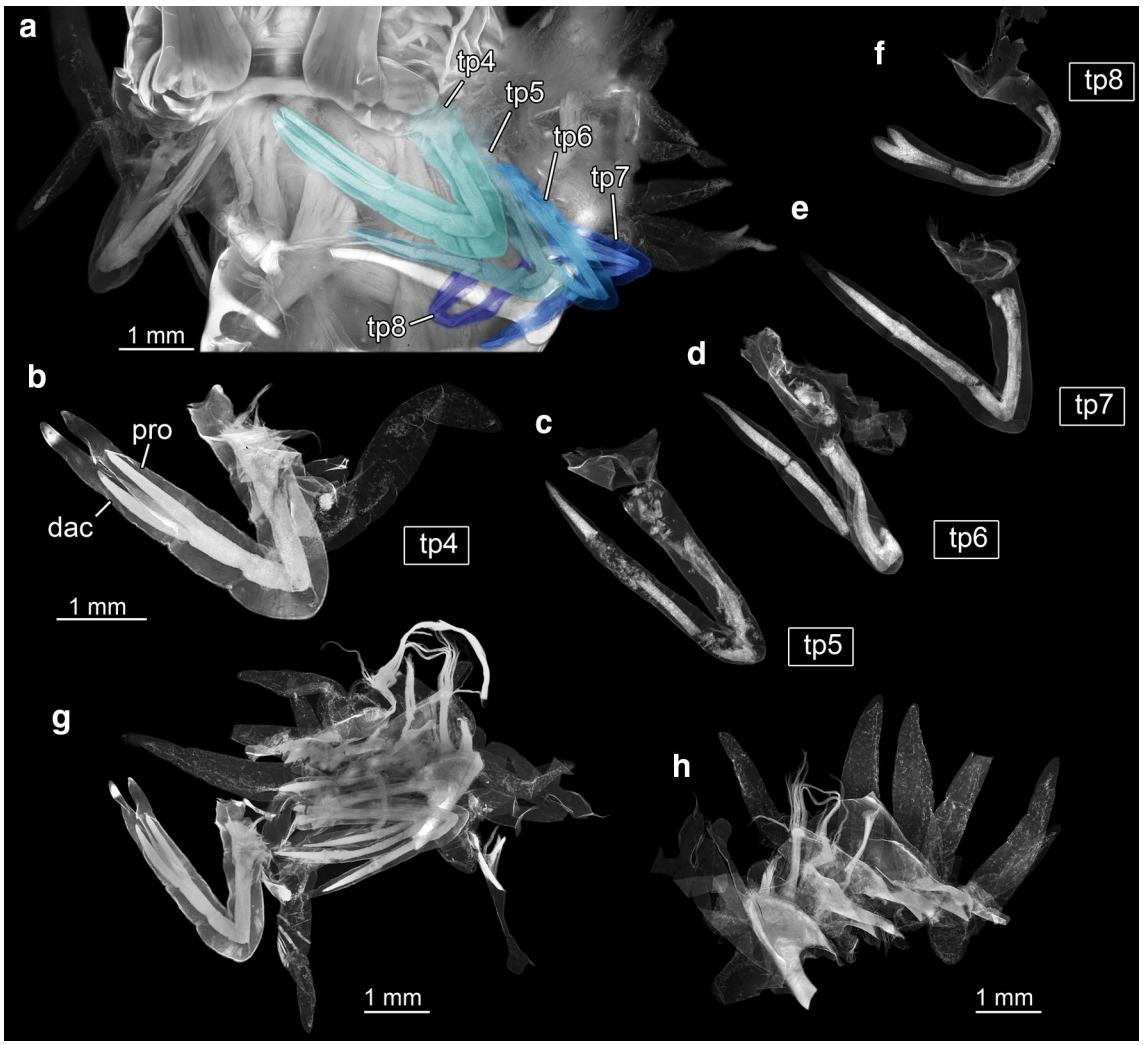

Fig. 24 Thoracopods of specimen B. Autofluorescence images (358 nm). **a** Colour-marked overview of thoracopods in situ in lateral view: thoracopod 4 (cyan), thoracopod 5 (cyan-blue), thoracopod 6 (light blue), thoracopod 7 (blue), thoracopod 8 (violet). **b**–**f** Isolated right thoracopods in posterior view. **b** Thoracopod 4. **c** Thoracopod 5. **d** Thoracopod 6. **e** Thoracopod 7. **f** Thoracopod 8. **g** Thoracopod 4 with gills. H. Isolated gills of thoracopod 4. Abbreviations: dac = dactylus; pro = propodus; tp 4–8 = thoracopod 4–8

capacities different from maxillipeds (weaker). No setae present.

Appendage of post-ocular segment 12 (thoracopod 7) Not (yet) differentiated into discrete elements embryonic in appearance; other structures not (yet) recognizable; distally spine-like; about the same size as preceding appendage (Fig. 24a, e, g). Next layer of cuticle visible; distinct gap between outer and inner cuticle. Appendage tube-shaped. Insertion area of the appendage located further dorsally than preceding appendage. Fluorescence capacities different from maxillipeds (weaker). No setae present.

Appendage of post-ocular segment 13 (thoracopod 8) Not (yet) differentiated into discrete elements tube-shaped, curved; embryonic in appearance; about the same size as preceding appendage (Fig. 24a, f, g). Fluorescence capacities different from maxillipeds (weaker). No setae present. With 2 spine-like elements; other structures not (yet) recognizable. Insertion area of the appendage located further dorsally than preceding appendage. Next layer of cuticle visible; distinct gap between outer and inner cuticle.

Gills (close to thoracopod insertions) Generally differentiated into knife-shaped structures; appear not (yet) functional; exact insertion area unclear (either proximally on the appendage or on the body proper close to the appendage insertion area) (Fig. 24h).

Appendage of post-ocular segment 14 (pleopod 1) Appendage not accessible.

Appendage of post-ocular segment 15 (pleopod 2) Appendage not (yet) differentiated into discrete elements tube-shaped, wider at the proximal part (Fig. 25a–d). Future differentiation into basipod, endopod, and exopod indicated. Next layer of cuticle visible; distinct gap between outer and inner cuticle. Basipod elongated, tube-shaped; longer than wide, about 3.5×.

Endopod tube-shaped; longer than wide, about 3×. Exopod tube-shaped; longer than wide, about 4×; longer than exopod, about 3×. Appendage with fluorescence capacities different from maxillipeds (weaker). No setae present.

Appendage of post-ocular segment 16 (pleopod 3) Not (yet) differentiated into discrete elements tube-shaped, wider at the proximal part; slightly larger than preceding appendage (Fig. 25a–d). Future differentiation into basipod, endopod, and exopod indicated. Next layer of cuticle visible; distinct gap between outer and inner cuticle. Basipod elongated, tube-shaped; about 5× longer than wide.

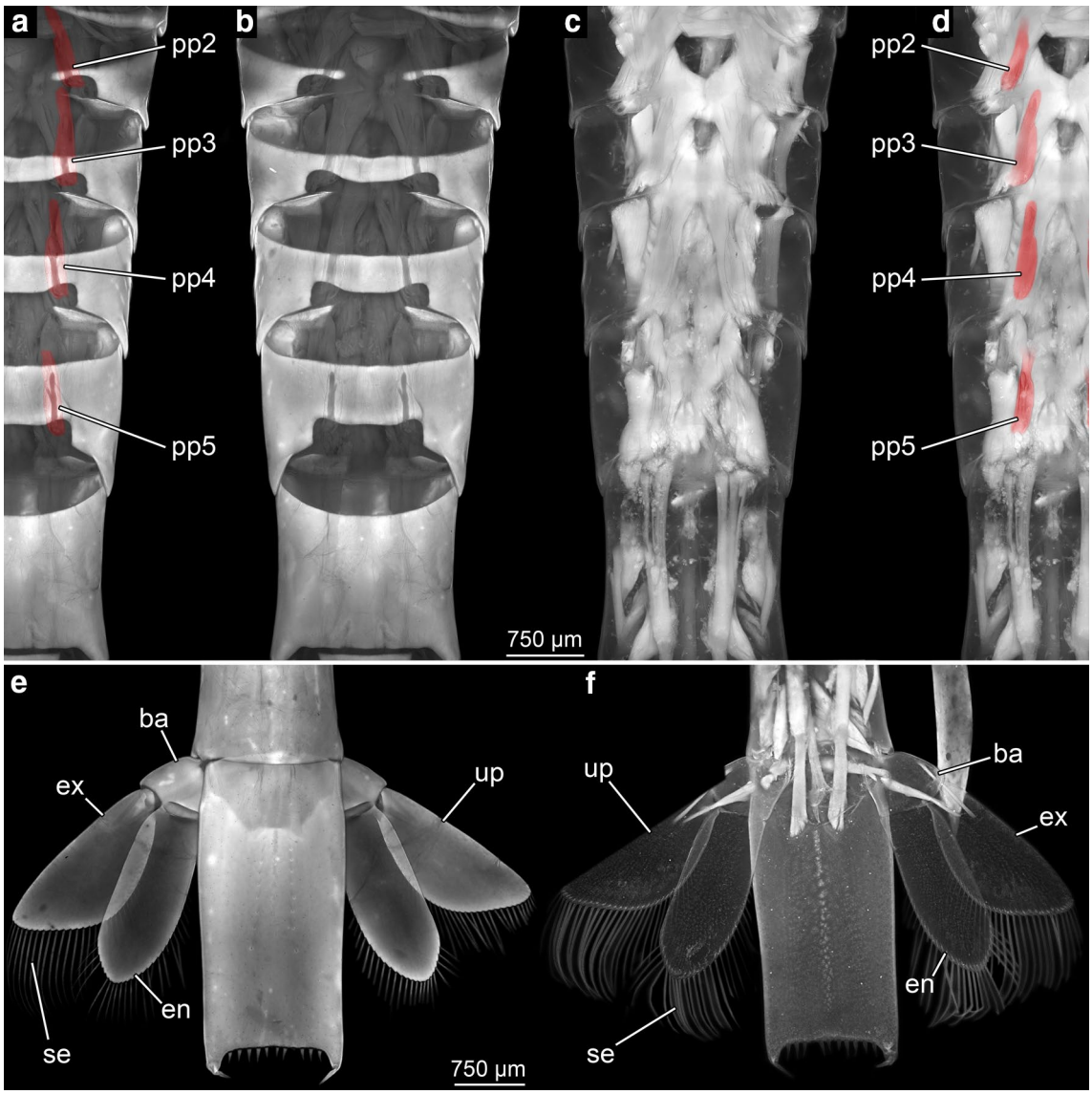

Fig. 25 Pleon and telson of specimen B. Autofluorescence images (**a**, **b**, **e** 358 nm; **c**, **d**, **f** 470 nm). **a**–**d** Overview of pleomeres with pleopods in ventral view. **a**, **d** Colour-marked overview; pleopods (red). **e**, **f** Overview of telson and uropods in dorsal view (**e**) and ventral view (**f**). *ba* basipod, *en* endopod, *ex* exopod, *pp 2–5* pleopod 2–5, *se* setae, *up* uropod

Endopod tube-shaped; longer than wide, about 3×. Exopod tube-shaped; longer than wide, about 3.5×. Appendage with fluorescence capacities different from maxillipeds (weaker). No setae present.

Appendage of post-ocular segment 17 (pleopod 4) Not (yet) differentiated into discrete elements tube-shaped, wider at the proximal part; slightly smaller than preceding appendage (Fig. 25a–d). Future differentiation into basipod, endopod, and exopod indicated. Next layer of cuticle visible; distinct gap between outer and inner cuticle. Appendage with fluorescence capacities different from maxillipeds (weaker). No setae present.

Appendage of post-ocular segment 18 (pleopod 5) Not (yet) differentiated into discrete elements tube-shaped, wider at the proximal part; slightly smaller than preceding appendage (Fig. 25a–d). Future differentiation into basipod, endopod, and exopod indicated. Next layer of cuticle visible; distinct gap between outer and inner cuticle.

Basipod tube-shaped; longer than wide, about 6×. Endopod tube-shaped; longer than wide, about 3×. Exopod tube-shaped; longer than wide, about 3×; longer than exopod, about 2×. Appendage fluorescence different from maxillipeds (weaker). No setae present.

Appendage of 19th post-ocular segment (uropod) Generally differentiated into basipod, endopod and exopod (Fig. 25e, f). Basipod more or less trapezoidal in anterior–posterior view; about as long as wide. Endopod blade-like; left and right about the same size (no asymmetry); longer than wide, about 2×; with about 26 setae medio-distally. Exopod more or less paddle-shaped; left and right about the same size (no asymmetry); longer than wide, about 2×; slightly larger than endopod; with about 32 setae medio-distally. Surface with no setae visible.

Gizzard (epidermal anterior part of gut) Sack-like structure with sclerotization on the left and right side, probably precursors of teeth; long setae in this area; short setae more in the middle (Fig. 26a, b). Gizzard subdivided into 3 parts. No distinct teeth (yet). Part 1 (median part) with numerous setae differing in length and width; long setae in the sclerotized part; distal end appears to pass into a Reusen-apparatus with lamellae and probably small teeth or spines (Fig. 26d, f). Lamellae not (yet) sclerotized. Distinct v-shaped sclerotization in the middle; posterior a field with lamellae. Part 2 (sidebar 1) with sclerotization on the lateral side; long setae in this area and short setae more in the middle (Fig. 26c). Part 3 (sidebar 2) with sclerotization in the middle; long setae in this area and short setae more in the middle (Fig. 26e).

Discussion

Comparison of both specimens

Both specimens share a number of characters, but also differ in certain aspects. It will, therefore, be necessary to compare them in detail to consider whether they might be conspecific or at least closely related. Differences and similarities are highlighted in the following paragraph.

Shield: Both specimens possess shields that are prominent and very large compared to the remaining body, but their shapes differ. The shield of specimen A is distinctly wider and slightly shorter than the shield of specimen B. The rostra of both specimens are very similar regarding their shape, but unlike specimen A, the rostrum of specimen B bears spines on each side of the lateral rim. Both shields show the muscle attachments for the mandibles, yet in specimen A these are arranged in two distinct lines in v-shape (Fig. 5b) while specimen B has a trapezoidal muscle attachment structure (Fig. 18a, d).

Both specimens have putative sensory organs (or glandular organs? See below for further discussion) on the middle line of their posterior shield region (circular field) and on the posterior region of the rostrum (trapezoidal field), each consisting of multiple pores (Figs. 5e, f, 18c, e, f). The strongly developed doublure extending from the ventral ridge in specimen A differs from the doublure of specimen B, in which it elongates into spines. The posterior rim of the shield of specimen A has a flat v-shaped notch, while specimen B has a rounded notch. The shield of specimen A has a cleft in the middle of the posterior rim elongating into a keel pointing anteriorly (Fig. 5b), while specimen B shows no cleft or keel on the entire shield. The shield of specimen A bears ventral, lateral, and latero-ventral ridges on the shield (Figs. 4a, 5a). Comparable ridges and keels are known in large larvae of mantis shrimps [11] and polychelidan lobsters [6, 34]. These might mechanically stabilise the large shields.

Compound eyes Although both larvae are of almost the same overall size, the compound eyes of specimen B are more than twice as large as those of specimen A (Fig. 3b, c vs. Figure 3e, f). Yet, specimen A has smaller ommatidia and therefore has about one-third more rows of ommatidia from the anterior to the posterior end of the eye than specimen B (Fig. 6 for specimen A; Fig. 19 for specimen B).

Both specimens have hexagonal facets, each surrounded by six other facets, in most regions of the eye; additionally, a distinct region with square-shaped facets, each surrounded by eight other facets, exists. At the transition between the two regions, some intermediate facets can be recognised as being surrounded by seven facets (Fig. 7).

In both specimens, the region with square-shaped facets is in the anterior part of their eyes. In specimen A,

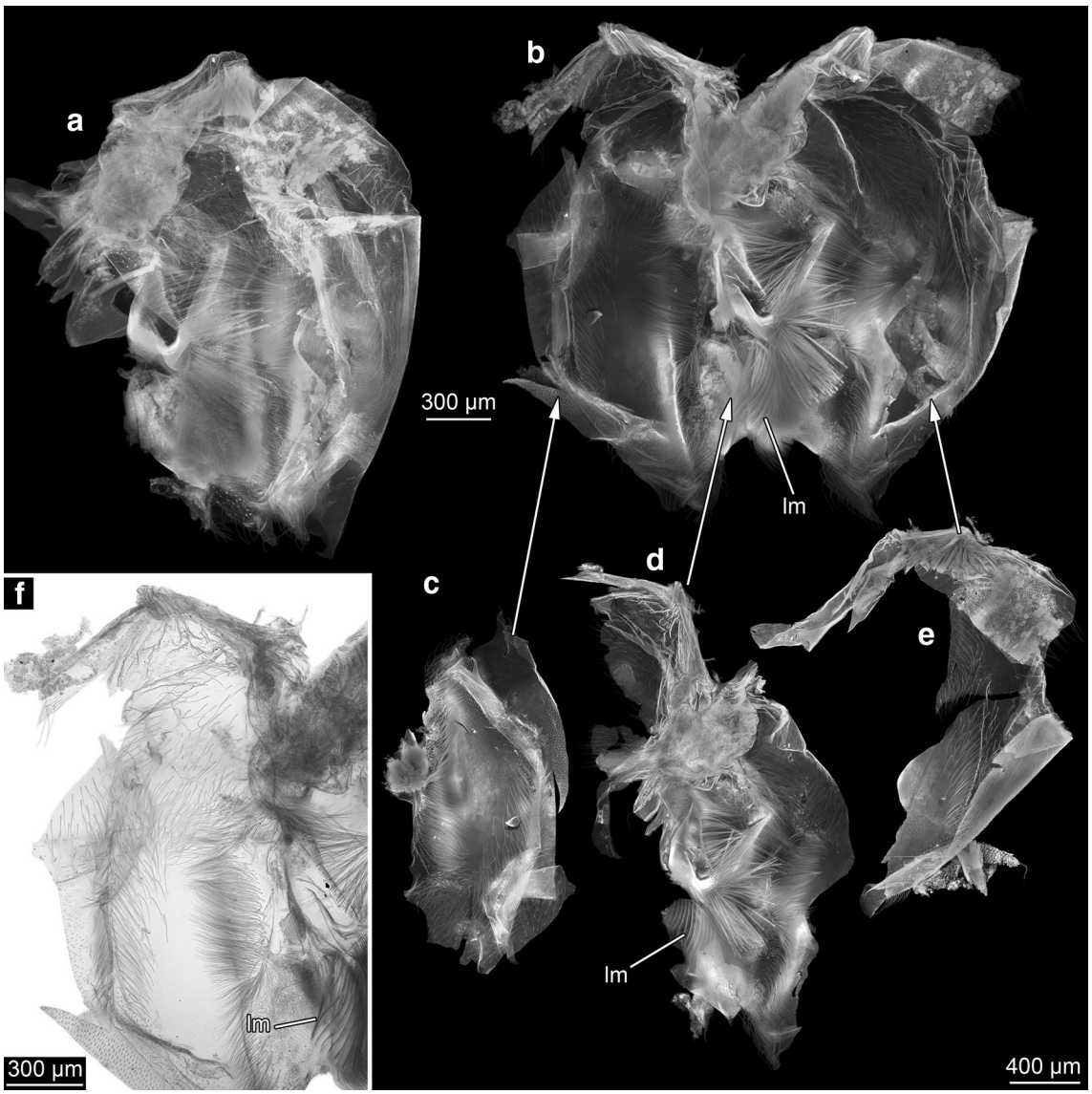

Fig. 26 Gizzard of specimen B. Autofluorescence images (**a**–**e** 358 nm) besides **f** which were recorded under transmitted white light conditions. **a** Overview of gizzard. **b** Overview of opened gizzard. **c** Isolated part 1. **d** Isolated part 2. **e** Isolated part 3. **f** Close-up on opened gizzard. *lm* lamellae

the region with the square-shaped facets is more on the middle and the ventral side of the eye, in specimen B the region with square-shaped facets is more on the dorsal side of the eye. Specimen A has more square-shaped facets than specimen B. Specimen A has a distinct pattern of pores on the dorsal region of the eyestalk. This resembles the sensory dorsal organ and therefore might represent a chemoreceptor (Figs. 5c, d, 6a, d).

Antennula and antenna: Regarding size and shape, both antennula and antenna are very similar in the two specimens (Figs. 8a–d, g, h, 9a–f, i–k for specimen A; Fig. 20a for specimen B). The main difference is the subdivision into two elements of the peduncle of the antennula (Figs. 8c, d, 9c, d for specimen A; Fig. 20a for specimen B), which is slightly more pronounced in specimen A. Such a subdivision of the antennula has been observed in many late larval stages of anomalan crustaceans (e.g. [35]). Also, the number of setae on flagellum 2 of the antennula is slightly lower in specimen A (Fig. 8e, f) than in specimen B (Fig. 20b, c). A conical structure proximally on the antenna bears a pore of a possible excretory organ, which is present in several crustacean larvae [6, 36]. This structure appears to be very similar for both studied specimens (Fig. 8i, j, 9e–h, j, k for specimen

A; Fig. 20d, e for specimen B). Unlike specimen B, specimen A bears a possible statocyst on the antenna (Fig. 9g, h; see further below for discussion).

Mouthparts: The labrum, mandible, paragnaths, maxillula, and maxilla seem to be rather similar in all anomalan larvae [37] (see Figs. 10, 11, 12, 21, 22). Endopod and exopod of maxillula and maxilla differ just slightly in shape, the distribution of setae and the number of structures is identical. The paragnaths also seem to be very similar with a little difference in overall shape (Figs. 10, 11 for specimen A; Fig. 21 for specimen B).

The most remarkable difference in the mouthparts is the shape of the mandible. Most anomalan larvae consume other small-sized metazoans; size, hardness, and muscular equipment of mandibles can be indicative of different types of food [38]. Specimen A has larger mandibles with stronger developed muscles and a smoother incisive part (Fig. 12) than specimen B (Fig. 21d). Hence it seems likely that both larvae originally exploited different food sources.

Maxillipeds: In both specimens, the maxillipeds (Figs. 13a, 14a for specimen A; Fig. 23a for specimen B) are fully functional, apparently used for swimming. However, they do not yet have a feeding and filtering function (as present in the adults). The maxillipeds 1 and 2 of both specimens are fully differentiated into coxa, basi-, endo- and exopod (Figs. 13b–e, 14B–E for specimen A; Fig. 23b–e for specimen B). The maxillipeds 3 of specimen A are differentiated into coxa, basipod, exopod and endopod, the latter being not fully developed yet, but already showing the future differentiation into five elements (Figs. 13f, g, 14f, g). The maxillipeds 3 of specimen B are even less far developed than those of specimen A, especially the endopod is barely recognisable as such (Fig. 23f, g).

Maxillipeds 1: of specimen B have a hook-shaped merus with one seta pointing towards the medial end. This structure might be used for grooming (Fig. 23b) by pulling the structures to be groomed through this corner (possibly "closing" it with the exopod). Comparable processes have been reported by Keiler and Richter [13].

Thoracopods 4-8: In both specimens, 5 pairs of posterior thoracopods (thoracopods 4 to 8) are already developed (Fig. 15 for specimen A; Fig. 24 for specimen B). All these thoracopods are embryonic, i.e. they lack distinct joints, setae, and spines, and have an overall rounded shape. Thoracopods of specimen A already show a slight differentiation into 4 to 6 elements; such an indication of future differentiation is not apparent in specimen B.

In both specimens, the distal part of thoracopod 4 is already differentiated into the fixed and the moveable finger of the chela 4. Also, on thoracopod 8 the distal part is already differentiated as a chela, yet more apparently in specimen B. In specimen B the next layer of cuticle inside the thoracopods is already well visible.

Pleomeres with pleopods: The pleon morphology of both specimens is also very similar. Yet, the pleomeres and especially the pleopods of specimen A appear further differentiated. The pleomeres of specimen A bear longer spines on each lateral side; also, the first pleomere is more pronounced, i.e. more easily visible than that of specimen B. The pleopods of specimen B have only just developed to be visible and are not yet differentiated (although the indication of the differentiation is visible), while the pleopods of specimen A are already slightly differentiated into basipod, endopod and exopod (Figs. 4a, b, 5a, b, 16 for specimen A; Figs. 8a, b, 25a–d for specimen B).

Uropods: Uropods of both specimens differ in size and shape. The shape of the uropods of specimen A is more tube-shaped, while the shape of the uropods of specimen B is paddle-shaped. Specimen A shows a left–right-asymmetry at both endopod and exopod (Fig. 16a–d), whereas specimen B has endopods and exopods of more or less the same size (Fig. 25e, f).

Telson: The two specimens differ significantly in the size and shape of their telson. Specimen A has a trapezoidal telson with one prominent paddle-shaped extension of the lateral rim on each side, both with a spine distally (Fig. 16a–d), while the telson of specimen B has an elongated rectangular structure with one small spine as extension of the lateral rim on each side (Fig. 25e, f).

Setae: Both specimens have setae on their body. In specimen A they are numerous on the dorsal and ventral side of the cephalothorax, the pleon, the telson, the antennae, and the uropods (e.g., Figure 9l). Specimen B has fewer setae on these structures and does not possess such setae on the ventral side, only on the dorsal side. Although the distribution of the setae is different for the studied specimens, their morphology is very similar. Two main types of setae can be observed: one type is the 'serrate' seta, mainly distributed on the lateral region of mouthparts; the second main group of setae on the mouthparts is the 'plumose' setae, which have a feather-like appearance (terminology from Garm [39]) (e.g. Fig. 22 for specimen B).

Foregut/Gizzard: The foregut morphology is very specific for the food habit of every species and its morphology shows interspecific variations, yet it may also provide clues for the evolutionary relationship of decapod groups [40–45]. The gizzards (posterior part of foregut) of both specimens appear very similar (Figs. 17, 26). Both gizzards are connected to the mouthparts by the oesophagus duct and appear sack-like. The gizzard seems roughly structured in three areas, each bearing numerous setae. The middle part seems to also bear lamellae and a heavily calcified arched structure (Fig. 17d for specimen A,

Fig. 26b for specimen B) most likely providing mechanical stability for the gizzard and most likely also acting as an attachment site for muscles.

Systematic interpretation

Meiuran adults never use their thoracopods for swimming, with the exception of crabs of the group Portunidae. During their entire zoea-larva stage, however, they use their maxillipeds to swim (more precisely, the exopods of these appendages) and directly switch swimming function to the pleopods, when moulting to the megalopa [16, 46]. In other groups of Decapoda, late larval forms use their thoracopods to move during their development before they use their pleopods, i.e. swimming function is gradually shifted from anterior to posterior [5, 15, 17].

The thoracopods of both specimens appear embryo-like, do not have an exopod, and are not sclerotised, while the pleopods are already developing. This feature identifies the specimens as larvae of Meiura [5]. Most zoea larvae of brachyuran meiurans bear a postero-dorsal spine on the shield [46], which is absent in both specimens. The eighth pair of thoracopods of the two specimens appears to be differentiating into grooming legs, indicative of an ingroup position within Anomala.

Among anomalan ingroups, the larvae roughly resemble larval forms of Lithodidae, Munididae, or Galatheidae. Lithodidae (king crabs) is a deep ingroup of Paguroidea (hermit crabs); Galatheidae is a possible ingroup of Munididae [47], which is an ingroup of Galatheoidea (squat lobsters; 2). Antennula and antenna have the shape of those of larvae of Munididae but do not match them regarding the size of antennulae and antennae compared to the rostrum. In known larvae of Munididae, antennulae and antennae are as long as the rostrum, yet, the antennula and the endopod of the antenna of specimens A and B are significantly shorter than the rostrum. This aspect is more similar to the condition in known larvae of Lithodidae. Larvae of Munididae (and hence also of Galatheidae) have comparably large compound eyes, as seen in specimen B, whereas specimen A has smaller eyes more comparable to larvae of Lithodidae.

Also, the shield provides differing phenotypes. Larvae of Munididae have a prominent rostrum. This feature is present in both specimens. Moreover, the rostrum of larvae of Munididae generally bears spines. Such spines are present on specimen B (Fig. 20a, f), but are absent on specimen A. Both specimens have rectangular shields covered with setae, like larval forms of Munididae. The distinct cleft in specimen A can also be seen in known larvae of this group.

The posterior rim of the shield of specimen A has a flat V-shaped notch at the posterior rim similar to larvae of Munididae, while specimen B has a rounded notch similar to larvae of Galatheidae. In addition, specimen A resembles larvae of Lithodidae concerning the shield structures: a keel, a lateral, a latero-ventral, and a ventral ridge, which extends to a well-developed doublure on its shield. The spine-like ventral teeth (Figs. 4c, 18g) are known in some larvae of Munididae and Porcellanidae and therefore might be characteristic for the larvae of those groups [48–53].

A part of the body that is similar to larvae of Munididae is the pleon. All pleomere tergites are rectangular in dorsal view and taper with every segment. They all have small spines at each lateral side, the only spine not represented on the analysed specimens is the spine in the middle of pleomere 6. Differentiated uropods in the size and shape present in the two specimens are almost only known in larvae of Munididae. Although specimen A has a left–right asymmetry and specimen B possesses uropods of almost the same size, overall morphology appears similar to larvae of Munididae.

Specimen A has a telson distantly resembling the telson of larvae of Lithodidae, at first sight. Yet, the telson of larvae of Lithodidae is truly fork-shaped, while the rim of the telson in specimen A is smoothly rounded. With the long paddle-like extensions, this telson resembles no posterior end of any already known larva. The rectangular shape of the telson of specimen B and the spines on each postero-lateral edge again resemble the telson as it has been described for megalopa larvae of Munididae [16].

Summing up, most characters indicate an ingroup position of Munididae for the two larval specimens. Yet, it becomes also clear that these larvae have a specialised morphology not known so far. As the two larvae are of similar size, but have significant morphological differences, it is unlikely that they represent the same species and only differ due to a different ontogenetic stage. The strong differences in the telson morphology make it even unlikely that they are very closely related. This may point to independent evolution of giant larvae within Munididae, but more data would be necessary to corroborate this.

Compound eyes

The compound eyes of both specimens seem to be unusual in certain aspects. Firstly, ommatidial size and opening angles of the corneae seem to be differentiated across the surface of a single compound eye. There are certain regions in the eyes where the ommatidia are smaller than in others and therefore have a higher density of ommatidia. This creates different regions with different performances, with which the larvae can see in various light intensities. Regions with a higher density of ommatidia have a higher resolution and the specimen can detect smaller objects. Regions with less, but larger ommatidia

have a higher exposure to light, making it possible for the specimen to see in a darker environment [54].

The largest opening angle between two ommatidia is positioned in the posterior region of the eyes in both specimens (Fig. 27b–d). In specimen B, the largest ommatidia are present in this region. In the anterior region, there is a higher density of ommatidia, creating a better resolution. The opening angles of the left eye and right eye ommatidia are overlapping and therefore creating two images of the same object. Objects in front of the larva will be detected by both eyes providing stereoscopic vision. To take advantage of this effect, the larvae can turn their eyes forward [7] (compare Fig. 27c, d).

The lateral part of the eyes of specimen B has an inward curvature. In this region, there is a similar density of ommatidia as in the anterior part. Also in this area, overlapping fields of view of neighbouring ommatidia might result in stereoscopic vision (Fig. 27a). Overall four different regions can be recognised, similar to the Cambrian (ca. 500 million years old) crustacean *Henningsmoenicaris scutula* [32, 55, 56]. The four region differentiation

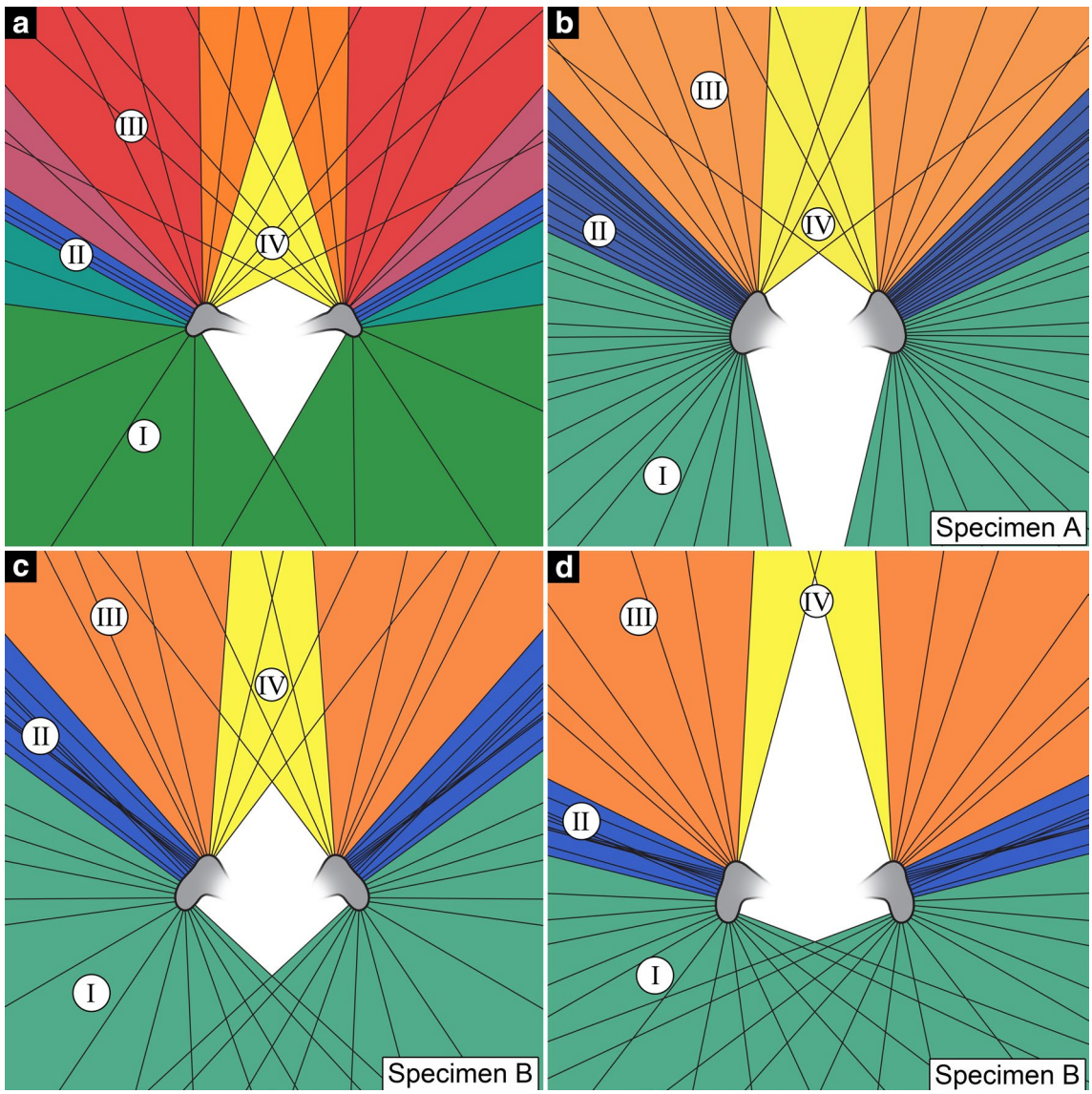

Fig. 27 Reconstruction of regions of different optical properties of compound eyes (following [32]). Region I: rear view, low resolution; region II: side view, very high resolution; III: anterior view, comparably high resolution; IV: anterior view with overlapping fields of view of both eyes resulting in stereoscopic vision in this region. **a** Example from a fossil crustacean (modified from [32]). **b** Specimen A. **c**, **d** Specimen B in different possible eye positions

might, therefore, be a more general phenomenon and widespread among planktic crustaceans.

Secondly, the compound eyes of both larvae have not only hexagonal facets, as typical for larval decapods, but already some areas with square-shaped facets surrounded by facets with intermediate morphologies. Comparing the distribution maps (Fig. 7) it is obvious that the two specimens have a different structure regarding the position of these regions. Yet, in both cases, the region with square-shaped facets is not close to the rim of the cornea. As has been shown by Vogt [57] and Nilsson [58] square-shaped facets are a good proxy for reflective superposition optics. In our specimens, an ontogenetic change from apposition to superposition within the "larval" part of the compound eye is thus the most plausible interpretation, though revealing an ontogenetic pattern of transition between two types of ommatidial optics is forcedly incomplete when, as in the present study, only one stage is available.

As there is no doubt that the compound eyes develop many more new ommatidia during metamorphosis from larva to adult via the megalopa stage, there seem to be two ways in which square-facetted ommatidia are formed: (i) from larval ommatidia with hexagonal facets by reconstruction; (ii) by de novo formation within the compound eye growth zone without hexagonal precursor.

Considering that there are two possible modes of how the eye might become transformed from an eye covered with hexagonal facets (larval apposition eye) to one with square-shaped facets (adult superposition eye) this is important. If we would expect that the square-shaped facets are added as new structures these should be concentrated at the rim of the cornea in which new facets are formed. A comparable pattern is known for the change in the eye of mantis shrimps [59]. However, in the two specimens investigated in this study the facets with the "new", i.e. square-shaped morphology, seem to be concentrated further away from the rim (although not entirely) indicating that at least some original hexagonal facets have been re-arranged into square-shaped ones.

Why is this of particular interest? Various studies have shown that accretion of new visual units in representatives of Euarthropoda with both ocellar eyes and tetraconate compound eyes takes place in a proliferation zone or morphogenetic field at the edge of the eye [60], while "intercalary" growth is restricted to addition of new cells in already existing eyes in non-tetraconate eyes. In our specimens, there is probably no intercalary growth, but intercalary reconstruction. As in the phantom midge *Chaoborus crystallinus* [24], this requires a second morphogenetic wave that induces the transformation without the proliferation of new cells. Where could this second wave come from? Most probably, the ontogenetic tools are used here that differentiate square-facetted ommatidia without hexagonal precursor, in other words, the toolbox for making adult ommatidia is already used in the larva, and this is a nice case of heterochrony or, more specifically, acceleration (or pre-displacement, or a combination of both) of a developmental pattern.

Earlier mappings of facet shape changes during ontogeny have shown that often, after some moults, all previously hexagonal ommatidia have square facets [61]. How is the situation for species studied in greater detail? In oplophorid caridean shrimps the transition proceeds either from anterior to posterior or starts in the lateral part of the compound eye [62]. In the true lobster *Nephrops norvegicus*, ommatidia mature in a gradient from posterior to anterior [63]. Thus it seems that there is no general scheme for the morphogenetic wave that produces square-shaped facets. Moreover, in some carideans, e.g. representatives of *Palaemon* (Palaemonidae) and *Eualus* (Hippolytidae) somewhat rudimentary, accessory eyes are found at the hind or upper edge of the compound eyes of the adults, and in some other malacostracans accessory visual neuropils next to the adult compound eye neuropils have been found ([64] for *Nebalia herbstii*; [65] for *Hippolyte inermis* and *Porcellana platycheles*). These structures are in similar positions as larval eyes and larval eye neuropils in holometabolan representatives of Insecta and similar eyes found in other arthropod main lineages [66]. In the future, it has to be solved how these partly different, partly even contradictory developmental patterns are related.

Sensory organ 1: dorsal organ

Crustaceans possess numerous different chemo- and mechanoreceptors on their cuticle. The 'sensory dorsal organ' is present in many crustaceans [67–69]. In both larvae, an anterior and a posterior field of pores can be differentiated indicating the still functional dorsal organ. Noticeably, specimen A possesses a comparable field of pores on the eye stalks. Similar structures have so far not been reported for decapod larvae or other arthropods.

Sensory organ 2: statocyst

Other important structures for crustaceans and mostly their larvae are special mechanoreceptors, the statocysts, generally a fluid-filled chitinous sack, which was formed by an invagination of the cuticle of the proximal area of the antenna [70], with a possible presence of a relatively dense mass composed by sand grains cemented together, the statolith [71, 72]. This organ is used by the larvae to maintain the orientation relative to gravity in water under low visibility conditions. These statocysts are in most larvae of Decapoda located proximally on the antennae [15, 73], but in most anomalan larvae they are

proximally on the antennulae [35, 74, 75]. Specimen A, however, appears to bear a possible statocyst in the proximal region of the antenna (Fig. 9g, h). This seems so far unknown for anomalan larvae.

Developmental status

Reptantians, lobsters, crabs, and relatives, normally have two larval phases: the planktic zoea phase, which can have up to ten stages, and the following megalopa phase, usually with only one stage. The pelagic zoea uses the exopods of its thoracopods to swim, while the megalopa swims with its pleopods [38]. Sometimes larvae show morphologies that cannot distinctly be identified as zoea or megalopa features, but morphologically being somewhere "in between" (early megalopa, e.g. [76–78]).

Both specimens mainly possess zoea characters, including the only weakly differentiated antennulae and antennae, the swimming-type maxillipeds, the embryo-like thoracopods, and the very little developed pleopods. The only structures in both specimens showing some further advanced structures are the eyes already possessing some square-shaped facets of the ommatidia. Specimen B additionally has a telson shape that seems more similar to some megalopa larvae than to most zoea larvae of anomalan crustaceans. This could be seen as an indication that specimen B should transform into a megalopa in the next moult. However, the morphology of the appendages indicated by the inner cuticle visible in the thoracopods and pleopods makes it more likely that the next stage is still zoea-like in appearance. Both larvae may represent therefore ultimate or at least penultimate zoea-phase larvae.

Size and macroplankton

Giant larvae occur in different crustacean ingroups, also in different ingroups of Decapoda [4]. Normally the zoea and megalopa reach a length of only a few millimeters, yet there are exceptions such as larvae of species of Aristidae (prawns) that measure up to 12 mm [79], of Polychelida that can even reach more than 100 mm in their megalopa stages [6, 34], or of Achelata with phyllosoma larvae of up to 150 mm leg span [5].

Both specimens investigated in this study are unusually large for anomalan larvae, as they both have a total length of 24 mm. Larvae of Porcellanidae ("false crabs") appear longer due to their very long spines, but clearly, have a smaller body compared to the two specimens described here. Therefore, the two specimens can be considered as the largest zoea-stage larvae in Meiura, being almost 10 mm longer than the so-far largest known one [12, 80]. Such large larvae should play an important role in the marine food web (being part of the macroplankton) and may exhibit important dispersal strategies. Although the report of only two specimens provides the impression that such larvae are rare, this is very likely a bias based on the scientific tradition of not or only rarely reporting larvae from plankton samples that cannot be identified to species. Similar recent finds of giant larvae are known from mantis shrimps [11]. Recognising groups with such large, possibly long-dispersal larvae is of importance for conservation biology. Our knowledge of macro-plankton is still very limited [81]. Crustacean larvae in this size fraction seem to be much more widespread concerning systematic groups but remain unrecognised [82]. With our report of the two giant larvae, we hope to trigger further research in this direction.

Conclusions

Summarising our observations:

- The two unusual larvae are most likely larvae of Munidida, i.e. squat lobsters.
- The two larvae possess eyes in the transformation from an apposition eye to a superposition eye, indicating that this restructuring process occurs not in a single moult, but over several moults.
- The ommatidia of the compound eyes seem to be rearranged to a new pattern, and not only regrow in a square order.
- The two larvae represent the largest so far known larval forms of meiuran crustaceans.
- Giant larvae seem to be more widespread systematically and more common than anticipated. Most likely they represent an important part of the macroplankton.

Acknowledgements

Laure Corbari, Paris, kindly helped with work in the collections and loan of the specimens. Free computer software was used in this study such as Combine ZM/ZP, OpenOffice, and others. We thank J. Matthias Starck and his work group for ongoing support.

Authors' contributions

CC, CH, JTH, LLF, and PG prepared the specimens and produced the images. CC, LLF, and PG arranged the figure plates and drafted the manuscript. CH, JTH and RRM conceived the study, participated in its design and coordination, and helped to draft the manuscript. All authors analysed the data. All authors read and approved the final manuscript.

Funding

This study was funded by the German Research Foundation under Ha 6300/3-2 (project 'Palaeo-Evo-Devo of Malacostraca') and by the Volkswagen Foundation in the frame of a Lichtenberg-Professorship. Additional funding was provided for LLF and PTG by Lehre@LMU. Research visits at MNHN Paris of CH and JTH have been made possible by grants from the European Commission's (FP 6) Integrated Infrastructure Initiative programme SYNTHESYS (FR-TAF-5175, FR-TAF-5181).

Availability of data and materials

All data generated or analysed during this study are included in this published article.

Ethics approval and consent to participate
Not applicable.

Consent for publication
Not applicable.

Competing interests
The authors declare that they have no competing interests.

Received: 19 July 2019 Accepted: 24 July 2020
Published online: 06 August 2020

References

1. Dussart BM. Les différentes catégories de plancton. Hydrobiologia. 1965;26:72–4.
2. Hays GC, Richardson AJ, Robinson C. Climate change and marine plankton. Trends Ecol Evol. 2005;20:337–44.
3. Sommer U, Stibor H. Copepoda–Cladocera–Tunicata: the role of three major mesozooplankton groups in pelagic food webs. Ecol Res. 2002;17:161–74.
4. Nagler C, Høeg JT, Haug C, Haug JT. A possible 150 million years old cirripede crustacean nauplius and the phenomenon of giant larvae. Contrib Zool. 2017;86:213–27.
5. Palero F, Clark PF, Guerao G. Achelata. In: Martin JW, Olesen J, Høeg JT, editors. Atlas of crustacean larvae. Baltimore: The Johns Hopkins University Press; 2014. p. 272–8.
6. Eiler SM, Haug JT, Haug C. Detailed description of a giant polychelidan eryoneicus-type larva with modern imaging techniques (Eucrustacea, Decapoda, Polychelida). Spixiana. 2016;39:39–60.
7. Haug JT, Audo D, Haug C, Abi Saad P, Petit G, Charbonnier S. Unique occurrence of polychelidan lobster larvae in the fossil record and its evolutionary implications. Gondwana Res. 2015;28:869–74.
8. Torres AP, Palero F, Santos A, Abelló P, Blanco E, Boné A, Guerao G. Larval stages of the deep-sea lobster *Polycheles typhlops* (Decapoda, Polychelida) identified by DNA analysis: morphology, systematic, distribution and ecology. Helgol Mar Res. 2014;68(3):379–97.
9. Ahyong ST, Baba K, Macpherson E, Poore GCB. A new classification of the Galatheoidea (Crustacea: Decapoda: Anomura). Zootaxa. 2010;2676:57–68.
10. Ahyong ST, Haug JT, Haug C. Stomatopoda. In: Martin JW, Olesen J, Høeg JT, editors. Atlas of crustacean larvae. Baltimore: The Johns Hopkins University Press; 2014. p. 185–9.
11. Haug C, Ahyong ST, Wiethase JH, Olesen J, Haug JT. Extreme morphologies of mantis shrimp larvae. Nauplius. 2016;24:e2016020.
12. Rudolf NR, Haug C, Haug JT. Functional morphology of giant mole crab larvae: a possible case of defensive enrollment. Zool Lett. 2016;2:17.
13. Keiler J, Richter S. Morphological diversity of setae on the grooming legs in Anomala (Decapoda: Reptantia) revealed by scanning electron microscopy. Zool Anzeiger. 2011;250:343–66.
14. Scholtz G, Richter S. Phylogenetic systematics of the reptantian Decapoda (Crustacea, Malacostraca). Zool J Linn Soc. 1995;113:289–328.
15. Anger K. The biology of decapod crustacean larvae. Crustacean Issues, vol. 14. Lisse: AA Balkema Publishers; 2001. p. 1–420.
16. Harvey A, Boyko CB, McLaughlin P, Martin JW. Anomura. In: Martin JW, Olesen J, Høeg JT, editors. Atlas of crustacean larvae. Baltimore: The Johns Hopkins University Press; 2014. p. 283–94.
17. Haug JT. Metamorphosis in crustaceans. In: Watling L, Thiel M, editors. Developmental biology and larval ecology. The natural history of the crustacea, vol. 7. Oxford: Oxford University Press; 2020.
18. Fincham AA. Ontogeny of anomuran eyes. Symp Zool Soc Lond. 1988;59:123–55.
19. Gaten E. Optics and phylogeny: is there an insight? The evolution of superposition eyes in the Decapoda (Crustacea). Contribut Zool. 1998;67:223–36.
20. Richter S. Evolution of optical design in the Malacostraca (Crustacea). P. In: Wiese K, editor. The Crustacean Nervous System. Berlin: Springer; 2002. p. 512–24.
21. Melzer RR. Optic lobes of the larval and imaginal scorpionfly *Panorpa vulgaris* (Mecoptera, Panorpidae): a neuroanatomical study of neuropil organization, retinula axons, and lamina monopolar cells. Cell Tissue Res. 1994;275:283–90.
22. Saltin BD. Further evidence for pre-metamorphosis larval eye reduction in the Holometabola (Insecta: Mecoptera: *Panorpa vulgaris* Imhoff and Labram, 1836). Contrib Entomol. 2015;65:105–11.
23. Williams BG, Greenwood JG, Jillett JB. Seasonality and duration of the developmental stages of *Heterosquilla tricarinata* (Claus, 1871) (Crustacea: Stomatopoda) and the replacement of the larval eye at metamorphosis. Bull Mar Sci. 1985;36:104–14.
24. Melzer RR, Paulus HF. Post-larval development of compound eyes and stemmata of *Chaoborus crystallinus* (De Geer, 1776) (Diptera: Chaoboridae): stage-specific reconstructions within individual organs of vision. Int J Insect Morphol Embryol. 1994;23:261–74.
25. Melzer RR, Zimmermann T, Smola U. Modification of dispersal patterns of branched photoreceptor axons and the evolution of neural superposition. Cell Mol Life Sci (Experientia). 1997;53:242–7.
26. Haug C, Mayer G, Kutschera V, Waloszek D, Maas A, Haug JT. Imaging and documenting gammarideans. Int J Zool. 2011. https://doi.org/10.1155/2011/380829.
27. Kerp H, Bomfleur B. Photography of plant fossils—new techniques, old tricks. Rev Palaeobot Palynol. 2011;166:117–51.
28. Haug JT, Haug C, Kutschera V, Mayer G, Maas A, Liebau S, Castellani C, Wolfram U, Clarkson ENK, Waloszek D. Autofluorescence imaging, an excellent tool for comparative morphology. J Microsc. 2011;244:259–72.
29. Rötzer MA, Haug JT. Larval development of the European lobster and how small heterochronic shifts lead to a more pronounced metamorphosis. Int J Zool. 2015;2015:345172.
30. Haug C, Shannon KR, Nyborg T, Vega FJ. Isolated mantis shrimp dactyli from the Pliocene of North Carolina and their bearing on the history of Stomatopoda. Bolétin de la Sociedad Geológica Mexicana. 2013;65:273–84.
31. Haug JT, Haug C, Ehrlich M. First fossil stomatopod larva (Arthropoda: Crustacea) and a new way of documenting Solnhofen fossils (Upper Jurassic, Southern Germany). Palaeodiversity. 2008;1:103–9.
32. Schoenemann B, Castellani C, Clarkson ENK, Haug JT, Maas A, Haug C, Waloszek D. The sophisticated visual system of a tiny Cambrian crustacean: analysis of a stalked fossil compound eye. Proc R Soc Lond B. 2012;279:1335–40.
33. Haug JT, Briggs DEG, Haug C. Morphology and function in the Cambrian Burgess Shale megacheiran arthropod *Leanchoilia superlata* and the application of a descriptive matrix. BMC Evol Biol. 2012;12:162.
34. Martin JW. Polychelida. In: Martin JW, Olesen J, Høeg JT, editors. Atlas of crustacean larvae. Baltimore: The Johns Hopkins University Press; 2014. p. 279–82.
35. Crain JA, McLaughlin PA. Larval, postlarval and early juvenile development in *Pagurus venturensis* Coffin, 1957 (Decapoda: Anomura: Paguridae) rared in the laboratory, with a redescription of the adult. Bull Mar Sci. 1993;53:985–1012.
36. Boxshall G, Jaume D. Antennules and antennae in crustacean. In: Watling L, Thiel M, editors. Functional morphology and diversity the natural history of the crustacea, vol. 1. Oxford: Oxford University Press; 2013. p. 199–236.
37. Abrunhosa FA, Kittaka J. Functional morphology of mouthparts and foregut of the last zoea, glaucothoe and first juvenile of the king crab *Paralithodes camtschaticus*, *P. brevipes* and *P. platypus*. Fish Sci. 1997;63:923–30.
38. Gonor SL, Gonor JJ. Feeding, cleaning, and swimming behavior in larval stages of porcellanid crabs (Crustacea: Anomura). Fish Bull. 1973;71(1):225–34.
39. Garm A. Revising the definition of the crustacean seta and setal classification systems based on examinations of the mouthpart setae of seven species of decapods. Zool J Linn Soc. 2004;142(2):233–52.
40. Allardyce BJ, Linton SM. Functional morphology of the gastric mills of carnivorous, omnivorous, and herbivorous land crabs. J Morphol. 2010;271(1):61–72.
41. Brösing A, Richter S, Scholtz G. The foregut-ossicle system of *Dromia wilsoni*, *Dromia personata* and *Lauridromia intermedia* (Decapoda, Brachyura, Dromiidae), studied with a new staining method. Arthrop Struct Dev. 2002;30(4):329–38.
42. Brösing A, Richter S, Scholtz G. Phylogenetic analysis of the Brachyura (Crustacea, Decapoda) based on characters of the foregut with establishment of a new taxon. J Zool Syst Evol Res. 2007;45(1):20–32.

43. De Jong-Moreau L, Casanova JP. The foreguts of the primitive families of the Mysida (Crustacea, Peracarida): a transitional link between those of the Lophogastrida (Crustacea, Mysidacea) and the most evolved Mysida. Acta Zoologica. 2001;82(2):137–47.
44. Reimann A, Richter S, Scholtz G. Phylogeny of the Anomala (Crustacea, Decapoda, Reptantia) based on the ossicles of the foregut. Zool Anzeiger J Compar Zool. 2011;250(4):316–42.
45. Williner V. Foregut ossicles morphology and feeding of the freshwater anomuran crab *Aegla uruguayana* (Decapoda, Aeglidae). Acta Zoologica. 2010;91(4):408–15.
46. Martin JW. Brachyura. In: Martin JW, Olesen J, Høeg JT, editors. Atlas of crustacean larvae. Baltimore: The Johns Hopkins University Press; 2014. p. 295–310.
47. Bracken-Grissom HD, Cannon ME, Cabezas P, Feldmann RM, Schweitzer CE, Ahyong ST, Felder DL, Lemaitre R, Crandall KA. A comprehensive and integrative reconstruction of evolutionary history for Anomura (Crustacea: Decapoda). BMC Evol Biol. 2013;13:128.
48. Christiansen ME, Anger K. Complete larval development of *Galathea intermedia* Lilljeborg reared in laboratory culture (Anomura: Galatheidae). J Crustac Biol. 1990;10(1):87–111.
49. Fujita Y, Baba K, Shokita S. Larval development of *Galathea amboinensis* (Decapoda: Anomura: Galatheidae) under laboratory conditions. Crust Res. 2003;32:79–97.
50. Hernández G, Bolaños J, Graterol K, Lira C. The larval development of *Petrolisthes politus* (Gray, 1831)(Crustacea: Decapoda: Porcellanidae) under laboratory conditions. Stud Neotrop Fauna Environ. 2000;35(2):143–56.
51. Konishi K, Saito T. Larvae of the deep-sea squat lobsters, *Agononida incerta* (Henderson, 1888) and *Munida striola* Macpherson and Baba, 1993 with notes on larval morphology of the family (Crustacea: Anomura: Galatheidae). Zool Sci. 2000;17(7):1021–9.
52. Roberts PE. Larvae of *Munida subrugosa* (White), 1847, from Perseverance Harbour, Campbell Island. J R Soc N Z. 1973;3(3):393–408.
53. Wehrtmann IS, Albornoz L, Véliz D, Pardo LM. Early developmental stages, including the first crab, of *Allopetrolisthes angulosus* (Decapoda: Anomura: Porcellanidae) from Chile, reared in the laboratory. J Crustac Biol. 1996;16(4):730–47.
54. Land MF, Nilsson DE. Animal eyes. Oxford: Oxford University Press; 2012.
55. Castellani C, Maas A, Haug C, Haug JT, Waloszek D. Isolated sponge spicules from the late Cambrian Alum Shale Formation ('Orsten' nodules) of Sweden. Bull Geosci. 2012;87:443–60.
56. Haug JT, Maas A, Waloszek D. †*Henningsmoenicaris scutula*, †*Sandtorpia vestrogothiensis* gen. et sp. nov. and heterochronic events in early crustacean evolution. Earth Environ Sci Trans R Soc Edinburgh. 2010;100:311–50.
57. Vogt K. Die Spiegeloptik des Flusskrebsauges. J Comp Physiol. 1980;135(1):1–19.
58. Nilsson D. Evolutionary links between apposition and superposition optics in crustacean eyes. Nature. 1983;302:818–21.
59. Feller KD, Cohen JH, Cronin TW. Seeing double: visual physiology of double-retina eye ontogeny in stomatopod crustaceans. J Comp Physiol A. 2015;201(3):331–9.
60. Harzsch S, Melzer RR, Müller CHG. Mechanisms of eye development and evolution of the arthropod visual system: the lateral eyes of Myriapoda are not modified insect ommatidia. Organ Div Evol. 2007;7:20–32.
61. Drach P, Tchernigovtzeff C. On the method of determination of larval stages and its general application to crustaceans. Vie Milieu. 1967;18(3A):595–607.
62. Gaten E, Herring PJ. Morphology of the reflecting superposition eyes of larval oplophorid shrimps. J Morphol. 1995;225:19–29.
63. Gaten E, Moss S, Johnson ML. The reniform reflecting superposition compound eyes of *Nephrops norvegicus*: optics, susceptibility to light-induced damage, electrophysiology and a ray tracing model. In: Johnson ML, Johnson MP, editors. Advances in marine biology, vol. 64. Amsterdam: Academic Press; 2013. p. 107–48.
64. Kenning M, Müller C, Wirkner CS, Harzsch S. The Malacostraca (Crustacea) from a neurophylogenetic perspective: new insights from brain architecture in *Nebalia herbstii* Leach, 1814 (Leptostraca, Phyllocarida). Zool Anzeiger. 2013;252:319–36.
65. Geiselbrecht H, Melzer RR. Nervous systems in 3D: A comparison of Caridean, anomuran, and brachyuran zoea-I (DECAPODA). J Exp Zool Part B. 2013;320(8):511–24.
66. Melzer RR. Persisting stemma neuropils in *Chaoborus crystallinus* (Diptera: Chaoboridae): development and evolution of a bipartite visual system. J Morphol. 2009;270(12):1524–30.
67. Barrientos Y, Laverack MS. The larval crustacean dorsal organ and its relationship to the trilobite median tubercle. Lethaia. 1986;19(4):309–13.
68. Lerosey-Aubril R, Meyer R. The sensory dorsal organs of crustaceans. Biol Rev. 2013;88(2):406–26.
69. Martin JW, Laverack MS. On the distribution of the crustacean dorsal organ. Acta Zool. 1992;73(5):357–68.
70. Nalbach HO. Multisensory control of eyestalk orientation in decapod crustaceans: An ecological approach. J Crustac Biol. 1990;10(3):382–99.
71. Cohen MJ. The function of receptors in the statocyst of the lobster *Homarus americanus*. J Physiol. 1955;130(1):9–34.
72. Prentiss CW. The otocyst of decapod Crustacea: its structure, development, and functions. Bull Mus Compar Zool. 1901;36(7):165–251.
73. Richter S, Scholtz G. Phylogenetic analysis of the Malacostraca (Crustacea). J Zool Syst Evol Res. 2001;39(3):113–36.
74. Komai T. A new species of the squat lobster genus *Munida* (Decapoda: Anomura: Munididae) from the North Pacific off Japan. Bull Natl Mus Nat Sci Ser A Suppl. 2011;5:101–8.
75. Komai T, Asakura A. *Pagurixus nomurai*, new species, and additional record of *Pagurixus maorus* (Nobili, 1906), hermit crabs from Kume-jima Island, the Ryukyus, Japan (Decapoda: Anomura: Paguridae). J Crustac Biol. 1995;15(2):341–54.
76. Haug JT, Haug C. An unusual fossil larva, the ontogeny of achelatan lobsters, and the evolution of metamorphosis. Bull Geosci. 2013;88:195–206.
77. Haug JT, Haug C, Waloszek D, Maas A, Wulf M, Schweigert G. Development in Mesozoic scyllarids and implications for the evolution of Achelata (Reptantia, Decapoda, Crustacea). Palaeodiversity. 2009;2:97–110.
78. Villamar DF, Brusca GJ. Variation in the larval development of *Crangon nigricauda* (Decapoda: Caridea), with notes on larval morphology and behavior. J Crustac Biol. 1988;8:410–9.
79. Bracken-Grissom HD, Felder DL, Vollmer NL, Martin JW, Crandall KA. Phylogenetics links monster larva to deep-sea shrimp. Ecol Evol. 2012;2(10):2367–73.
80. Martin J, Ormsby B. A large brachyuran-like larva of the Hippidae (Crustacea: Decapoda: Anomura) from the Banda Sea, Indonesia: the largest known zoea. Proc Biol Soc Wash. 1991;104(3):561–8.
81. Pierrot-Bults AC, Van der Spoel S. Macrozooplankton diversity: how much do we really know? Zoologische Verhandelingen. 2003;345:297–312.
82. Haug JT, Haug C. A new glimpse on Mesozoic zooplankton—150 million-year-old lobster larvae. PeerJ. 2017;5:e2966.

Publisher's Note